Wavelet analysis, from the line to the two-sphere

J-P. Antoine

Institut de Physique Théorique, Université catholique de Louvain
B-1348 Louvain-la-Neuve, Belgium

International Max Planck Research School on Physical Processes
in the Solar System and Beyond

Max Planck Institute for Solar System Research

Katlenburg-Lindau, May 8-9, 2008

INTRODUCTION

In real life :

- nonstationary signals
- wide spectrum of frequencies
- often correlation (ex. human voice):
  - HF $\leftrightarrow$ short duration, well localized in time
  - LF $\leftrightarrow$ long duration

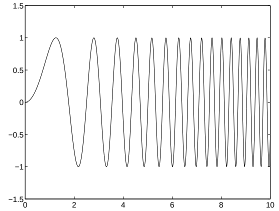

A nonstationary signal (chirp)

Traditional tool : Fourier transform

$$s(x) \quad \leftrightarrow \quad \widehat{s}(\xi) = \frac{1}{\sqrt{2\pi}} \int_{-\infty}^{\infty} e^{-i\xi x} s(x)\, dx$$

- no time localization : when does the $\widehat{s}(\xi)$ component occur ?
- very uneconomical : (almost) flat signal (no information!) requires summation of infinite series or calculation of integral
- very unstable : tiny perturbation $\Rightarrow$ Fourier spectrum completely perturbed (FT is global)

Effect of a localized perturbation

- A pure sine wave and the same with two delta perturbations added

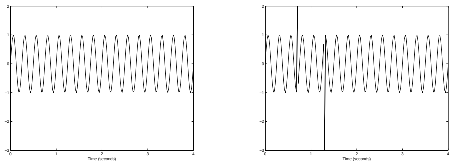

- The respective Fourier transforms

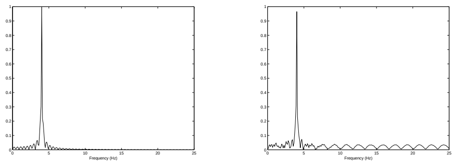

- The localized perturbations are completely delocalized in Fourier space !
- Conclusion : Fourier analysis is not sufficient !

Time-frequency representation

- Solution : Time-frequency representation
- Two parameters are needed :
  - frequency : which one ? $\longleftarrow$ a
  - time : when ? $\longleftarrow$ b
- General linear time-frequency transform :

$$s(x) \mapsto S(b,a) = \int_{-\infty}^{\infty} \overline{\psi_{b,a}(x)}\, s(x)\, dx,$$

where $\psi_{b,a}$ is the analyzing function.

- Example : Musical score !

A traditional time-frequency representation of a signal
(from Mozart's Don Giovanni, Act 1)

Two simple solutions

- *Windowed Fourier transform or Gabor transform*

$$\psi_{b,a}(x) = e^{i(x-b)/a}\, \psi(x-b) \quad : \quad a = \text{modulation},\ b = \text{translation}$$

$$(1/a \simeq \text{frequency})$$

- *Wavelet transform*

$$\psi_{b,a}(x) = \frac{1}{\sqrt{a}}\, \psi\left(\frac{x-b}{a}\right) \quad : \quad a = \text{scaling},\ b = \text{translation}$$

- What is the difference between the two?

Two simple solutions

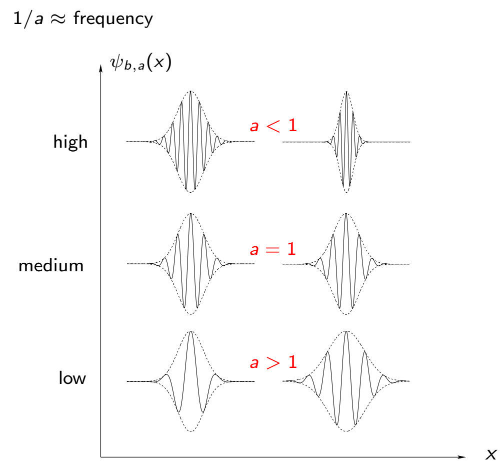

The function $\psi_{b,a}(x)$ for different values of the scale parameter a :
in the case of the Windowed Fourier Transform (left);
in the case of the wavelet transform (right)

Three stages of WT

- Continuous WT (CWT)

$$S(b,a) = |a|^{-1/2} \int_{-\infty}^{\infty} \overline{\psi\left(\frac{x-b}{a}\right)}\, s(x)\, dx, \quad a \neq 0,\ b \in \mathbb{R}$$

  . all values of a and b : useful for feature detection (often $a > 0$)

- Discretization of CWT
  . discretization needed for numerical implementation
  . choice of sampling grid
  . no orthonormal bases, only frames (redundant representation)

- Discrete WT (DWT)
  . preselected grid (dyadic)
  . (bi)orthonormal bases from multiresolution analysis
  . good for data compression

Three stages of WT

- Note :
(discretized) CWT incompatible with DWT, totally different philosophies

- Analogy :

CWT	$\Leftrightarrow$	Fourier integral
discretized CWT	$\Leftrightarrow$	Fourier series
DWT	$\Leftrightarrow$	discrete FT

WAVELET ANALYSIS OF 1-D SIGNALS

The Continuous WT in 1-D

- Basic formulas

$$\begin{aligned} S(b,a) &= \langle \psi_{b,a} | s \rangle \\ &= |a|^{-1/2} \int_{-\infty}^{\infty} \overline{\psi\left(\frac{x-b}{a}\right)}\, s(x)\, dx \\ &= |a|^{1/2} \int_{-\infty}^{\infty} \overline{\widehat{\psi}(a\xi)}\, \widehat{s}(\xi)\, e^{i\xi b}\, d\xi \end{aligned}$$

$a \neq 0,\ b \in \mathbb{R}$: time-scale plane $\mathbb{R}^2_*$

- Conditions on analyzing wavelet ψ

(i) $\psi,\ \widehat{\psi} \in L^2$

(ii) ψ admissible : $c_\psi \equiv 2\pi \int_{-\infty}^{\infty} \frac{|\widehat{\psi}(\xi)|^2}{|\xi|}\, d\xi < \infty$

which essentially reduces to a zero mean condition

$$\widehat{\psi}(0) = 0 \iff \int_{-\infty}^{\infty} \psi(x)\, dx = 0$$

The Continuous WT in 1-D

(iii) ψ and $\widehat{\psi}$ well localized : $\psi \in L^1 \cap L^2$ or better
$\Rightarrow$ good bandpass filtering in x and ξ

(iv) Vanishing moments: $\displaystyle\int_{-\infty}^{\infty} x^n\, \psi(x)\, dx = 0, \;\; n = 0, 1, \dots N$
$\Rightarrow$ ψ blind to polynomials of degree $\leqslant N$ (smooth part of signal)
$\Rightarrow$ better detection of singularities

(v) ψ progressive : $\widehat{\psi}$ real and $\widehat{\psi}(\xi) = 0$ for $\xi < 0$ (analytic signal)

Note : one takes often $a > 0$ (positive dilation factor only)

$\Rightarrow$ slightly different admissibility condition :

$$c_\psi \equiv 2\pi \int_0^\infty d\xi\, \frac{|\widehat{\psi}(\xi)|^2}{|\xi|}\, d\xi = 2\pi \int_{-\infty}^0 \frac{|\widehat{\psi}(\xi)|^2}{|\xi|}\, d\xi < \infty$$

(equality automatic if ψ real)

Two common wavelets

The Mexican hat wavelet

$$\psi_H(x) = (1 - x^2)\, e^{-\frac{1}{2}x^2}$$
$$\widehat{\psi}_H(\xi) = \xi^2\, e^{-\frac{1}{2}\xi^2}$$

. real
. admissible
. not progressive
. 2 vanishing moments $n = 0, 1$

The Morlet wavelet

$$\psi_M(x) = e^{i\xi_o x}\, e^{-x^2/2\sigma_o^2} + c(x)$$
$$\widehat{\psi}_M(\xi) = \sigma_o\, e^{-[(\xi-\xi_o)\sigma_o]^2/2} + \widehat{c}(\xi)$$

. complex
. admissible with correction term
. correction term negligible for $\sigma_o\xi_o \geqslant 5.5$
. not progressive

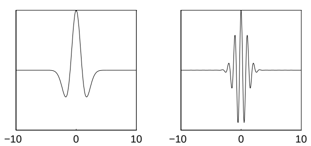

(left) Mexican hat or Marr wavelet;
(right) Real part of the Morlet wavelet, for $\xi_o = 5.6$

Localization properties and interpretation

Assume

num supp $\psi(x)$ $\sim$ L around 0
num supp $\widehat{\psi}(\xi)$ $\sim$ Ξ around ξ_o

Then

num supp $\psi_{b,a}(x)$ $\sim$ aL around b
num supp $\widehat{\psi}_{b,a}(\xi)$ $\sim$ Ξ/a around ξ_o/a

Therefore

- if $a \gg 1, \psi_{b,a}$ = wide window (long duration),
  $\widehat{\psi_{b,a}}$ peaked around small frequency ξ_o/a:
  $\Rightarrow$ sensitive to low frequencies (rough analysis)
- if $a \ll 1, \psi_{b,a}$ = narrow window (short duration),
  $\widehat{\psi_{b,a}}$ wide and centered around high frequency ξ_o/a:
  $\Rightarrow$ sensitive to high frequencies (small details)

Localization properties and interpretation

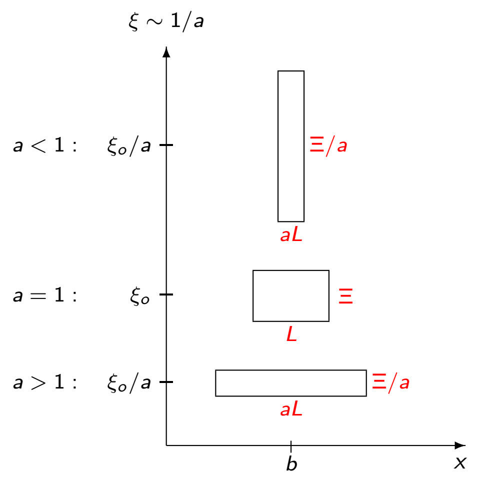

Support properties of $\psi_{b,a}$ and $\widehat{\psi_{b,a}}$

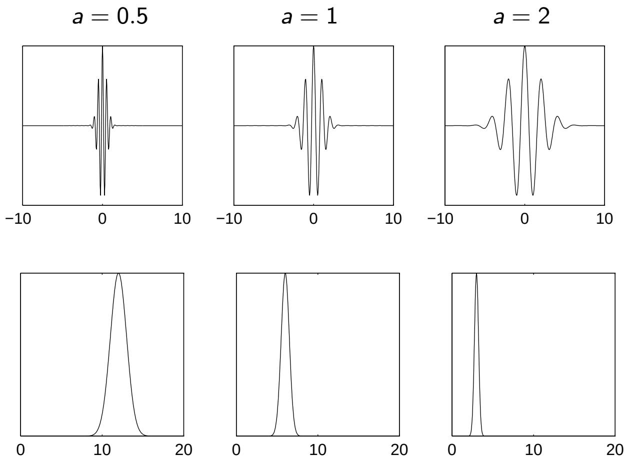

Support properties of the Morlet wavelet ψ_M:
for $a = 0.5, 1, 2$ (left to right), $\psi_{b,a}$ has width 3, 6, 12, respectively (top),
while $\widehat{\psi_{b,a}}$ has width 3, 1.5, 0.75, and peaks at 12, 6, 3 (bottom)

WT = zero mean filter (convolution) + localization properties $\Rightarrow$

- CWT = local filtering in time (b) and scale (a)

$$S(b,a) \not\approx 0 \quad \Longleftrightarrow \quad \psi_{b,a}(x) \approx s(x)$$

- CWT = mathematical microscope
  optics ψ, position b, magnification $1/a$
- CWT works at constant relative bandwidth : $\Delta\xi/\xi$ = const
- $\Rightarrow$ CWT = singularity detector and analyzer

For ψ admissible, the CWT $W_\psi : s(x) \mapsto S(b,a)$ is a linear map, with the following properties:

- Covariance under translation and dilation

$$W_\psi : s(x - x_o) \mapsto S(b - x_o, a)$$

$$W_\psi : \frac{1}{\sqrt{a_o}}\, s\left(\frac{x}{a_o}\right) \mapsto S\left(\frac{b}{a_o}, \frac{a}{a_o}\right)$$

- Energy conservation

$$\int_{-\infty}^{\infty} |s(x)|^2\, dx = c_\psi^{-1} \iint_{\mathbb{R}^2_*} |S(b,a)|^2\, \frac{da\, db}{a^2}$$

$\Rightarrow$ $|S(b,a)|^2$ = energy density in half-plane

$\Longleftrightarrow$ W_ψ = isometry from space of signals $L^2(\mathbb{R})$ onto closed subspace $\mathcal{H}_\psi$ of $L^2(\mathbb{R}^2_*, da\, db/a^2)$ = space of transforms

$\Rightarrow$ W_ψ invertible on its range $\mathcal{H}_\psi$ by adjoint map, i.e.

- Reconstruction formula

$$s(x) = c_\psi^{-1} \iint_{\mathbb{R}^2_*} \psi_{b,a}(x)\, S(b,a)\, \frac{da\, db}{a^2}$$

$\Rightarrow$ linear superposition of wavelets $\psi_{b,a}$ with coefficients $S(b,a)$

- Projection $P_\psi : L^2(\mathbb{R}^2_*, da\, db/a^2) \to \mathcal{H}_\psi$ is an integral operator, with kernel

$$K(b', a'; b, a) = c_\psi^{-1}\, \langle \psi_{b',a'} | \psi_{b,a} \rangle$$

K = autocorrelation function of ψ, reproducing kernel

$\Rightarrow$ $f \in L^2(\mathbb{R}^2_*, da\, db/a^2)$ is the WT of a certain signal iff it satisfies the reproduction property

$$f(b', a') = c_\psi^{-1} \iint_{\mathbb{R}^2_*} \langle \psi_{b',a'} | \psi_{b,a} \rangle\, f(b,a)\, \frac{da\, db}{a^2}$$

$\Rightarrow$ the CWT is a highly redundant representation !

$\Rightarrow$ Full information contained is small subset of half-plane :

- Lines of local maxima : ridges
- Discrete subset $\Rightarrow$ frames

- Real life signals often entangled and noisy, WT difficult to interpret
- But the energy density $|S(b,a)|^2$ is usually well concentrated, around lines of local maxima = ridges

  Skeleton = set of ridges

  Result : $S(b,a)\restriction_{\text{skeleton}}$ contains essentially the whole information
  $\Rightarrow$ Exploit redundancy by reducing WT to its skeleton
- Detecting singularities in signals : vertical ridges
  Application : estimating the strength of singularities $\equiv$ local Hölder regularity

$$s(x-x_o) \sim (x-x_o)^\alpha + \ldots, \quad \text{for } x \sim x_o$$

  + covariance property of the CWT under dilation
  $\Rightarrow$ along ridge, $|S(b,a)|$ behaves as a^α
  $\Rightarrow$ slope of plot of $\log|S(b,a)|$ vs. $\log a$ gives regularity index α

- Detecting characteristic frequencies in signals : horizontal ridges
  - Many signals are well approximated by a superposition of simple spectral lines:

$$s(x) = \sum_{n=1}^{N} A_n(x)\, e^{i\xi_n x}, \quad A_n(x) \text{ slowly varying amplitude}$$

  - By linearity, the WT is a sum of terms, $S(b,a) = \sum_n S_n(b,a)$
  - To first order, one gets $S(b,a) \simeq \sum_{n=1}^{N} \widehat{\psi}(a\xi_n) s_n(b)$
  - Assume $\widehat{\psi}(\xi)$ has a unique maximum in frequency space at $\xi = \xi_o$ and frequencies ξ_n are sufficiently far away from each other
  - Then $S_n(b,a)$ is localized on the scale $a_n = \xi_o/\xi_n$
    $\Rightarrow$ along the line of maxima $a = a_n$, called the nth horizontal ridge, the CWT is approximately proportional to the nth spectral line:

$$S(b,a_n) \simeq s_n(b)\, \widehat{\psi}(\xi_o)$$

  - Same reasoning for more general spectral lines (asymptotic signal)

$$s_n(x) = A_n(x)\, e^{i\phi_n(x)}, \quad A_n(x) \text{ slowly varying w.r. to } \phi_n(x)$$

  Typical example : NMR spectra

Wavelet analysis of a discontinuous signal with a Mexican hat wavelet

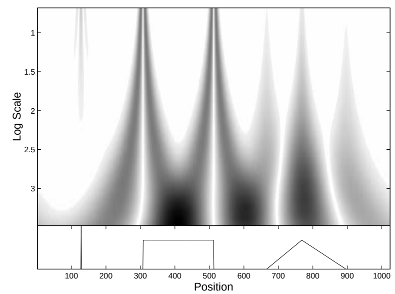

Wavelet transform

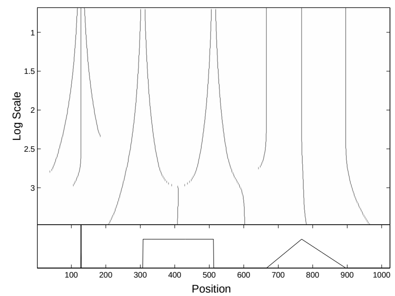

Skeleton of the same

Analysis of a rebound signal, with a Mexican hat wavelet

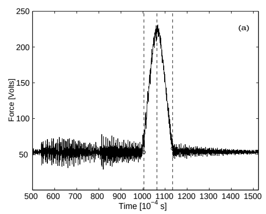

The signal and the points detected by the respective ridges

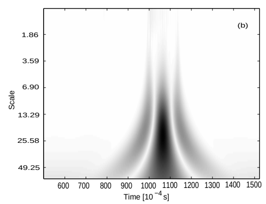

The modulus of the CWT

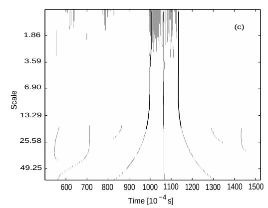

The corresponding skeleton

Analysis of a rebound signal, with a Morlet wavelet

Horizontal ridges

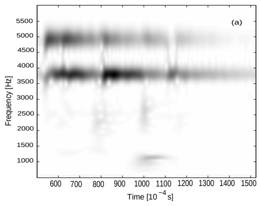

The modulus of the CWT

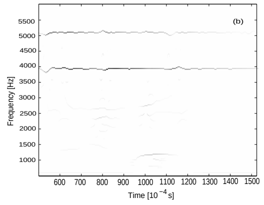

The corresponding skeleton

For applications, one has to choose an adequate wavelet : the choice depends on problem at hand !

- Detection of singularities
  - Phase irrelevant $\Rightarrow$ real wavelet
  - Need characterization of singularity strength
    $\Rightarrow$ derivative of Gaussian

$$\psi_G^{(n)}(x) = \left(\frac{d}{dx}\right)^n e^{-\frac{x^2}{2\sigma^2}} : \quad n \text{ vanishing moments}$$

    - $n = 1$: simplest case
    - $n = 2$: Mexican hat : erases linear trends
- Spectral analysis
  - Detection of characteristic frequencies, denoising or rephasing of spectra,...
  - Phase essential
    - Modulus/phase representation of CWT
    - Use of instantaneous frequency

    $\Rightarrow$ Morlet wavelet

$$\psi_M(x) = e^{i\xi_o x}\, e^{-x^2/2\sigma^2} + c(x), \quad c(x) \text{ negligible for } \sigma\xi_o \geqslant 5.5$$

- In both cases, σ controls resolution in time and in frequency $\Rightarrow$ adapt width σ to signal at hand

- Noise removal in signals
  removal of undesirable noise in signals by subtraction and reconstruction
- Sound and acoustics
  musical synthesis, speech analysis (formant detection), disentangling of underwater acoustic wavetrain
- Geophysics
  analysis of microseisms in oil prospection, gravimetry (fluctuations of the local gravitational field), seismology, geomagnetism (fluctuations of the Earth magnetic field), astronomy (fluctuations of the length of the day, variations of solar activity, measured by the sunspots, etc)
- Fractals, turbulence (1-D and 2-D)
  diffusion limited aggregates, arborescent growth phenomena, identification of coherent structures in developed turbulence

- Atomic physics
  analysis of harmonic generation in laser-atom interaction
- Spectroscopy
  NMR spectroscopy : subtraction of spectral lines, noise filtering
- Medical and biological applications
  analyzing or monitoring of EEG, VEP, ECG; long-range correlations in DNA sequences
- Analysis of local singularities
  determination of local Hölder exponents of functions
- Shape characterization
  robotic vision : CWT of contour of an object treated as a complex curve in the plane
- Industrial applications
  monitoring of nuclear, electrical or mechanical installations ; analysis of behavior of materials under impact

Physical applications of CWT

Noise removal (filtering) in a signal

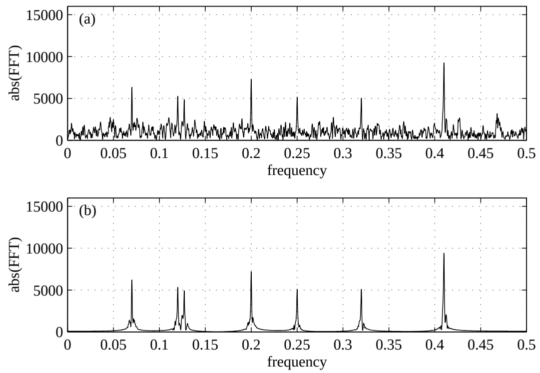

- (Top) noisy signal : original NMR spectrum
- (Bottom) denoised signal : reconstructed spectrum after noise removal

Physical applications of CWT

Suppression of unwanted (water) peak in a NMR spectrum

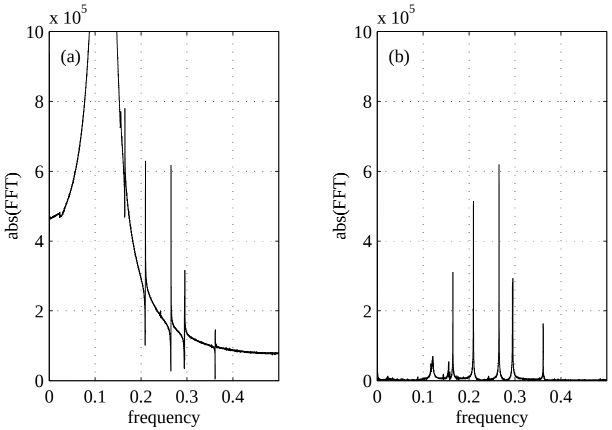

- (Left) original NMR spectrum
- (Right) reconstructed spectrum after water peak removal

Physical applications of CWT

Detection of discontinuities in a signal

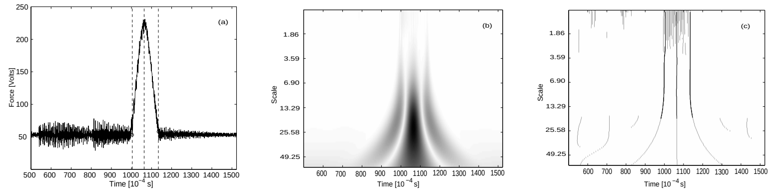

(a) (b) (c)

Fall of a striker on a plastic disk : analysis of rebound signal with a Mexican hat wavelet

(a) Signal : rebounding striker acceleration (= force) and discontinuity points to be detected
(b) Absolute value of the CWT of signal
(c) Corresponding skeleton

Discretization of CWT

- CWT must be discretized for numerical implementation
- Choice of sampling grid: discrete lattice $\Gamma = \{a_j, b_{j,k}, j, k \in \mathbb{Z}\}$ yields good discretization if

$$s = \sum_{j,k \in \mathbb{Z}} \langle \psi_{jk}, s \rangle \widetilde{\psi}_{jk}$$

with $\psi_{jk} \equiv \psi_{b_{j,k},a_j}$ and $\widetilde{\psi}_{jk}$ explicitly constructible from ψ_{jk}

- Common choice : dyadic grid $a_j = 2^{-j}$, $b_{j,k} = k \cdot 2^{-j}$

$$\psi_{jk}(x) = 2^{j/2} \psi(2^j\, x - k), \quad j, k \in \mathbb{Z}$$

- Usually leads to frames, not bases

The dyadic lattice

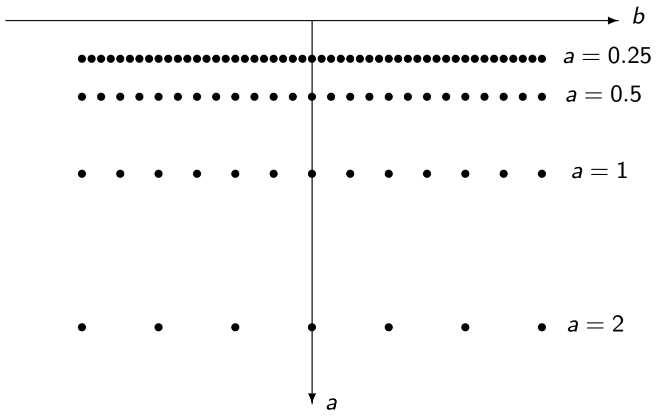

Frames

- Relevant concept : $\{\psi_{jk}\}$ is a frame in $\mathcal{H}$ if $\exists\, \mathrm{m} > 0, \mathrm{M} < \infty$ s.t.

$$\mathrm{m}\, \|s\|^2 \;\leqslant\; \sum_{j,k\,\in\,\mathbb{Z}} |\langle \psi_{jk} | s\rangle|^2 \;\leqslant\; \mathrm{M}\, \|s\|^2$$

  - m, M = frame bounds
  - $\mathrm{m} = \mathrm{M} \neq 1$: tight frame
  - $\mathrm{m} = \mathrm{M} = 1$ and $\|\psi_{jk}\| = 1$: orthonormal basis

- Question : given wavelet ψ, find lattice Γ s.t. $\{\psi_{jk}\}$ is a good frame, i.e. such that $\left|\frac{\mathrm{M}}{\mathrm{m}} - 1\right| \ll 1$

- Solution : lattice adapted to geometry, e.g. dyadic lattice
  Result : Mexican hat and Morlet wavelets give good, nontight frames

- $\Longrightarrow$ need another approach to get a basis : DWT, based on multiresolution analysis

The discrete WT (DWT)

- Multiresolution analysis of $L^2(\mathbb{R})$ = increasing sequence of closed subspaces

$$\ldots \subset V_{-2} \subset V_{-1} \subset V_0 \subset V_1 \subset V_2 \subset \ldots$$

  with $\bigcap_{j\,\in\,\mathbb{Z}} V_j = \{0\}$ and $\bigcup_{j\,\in\,\mathbb{Z}} V_j$ dense in $L^2(\mathbb{R})$, and such that

  (1) $f(x) \in V_j \Leftrightarrow f(2x) \in V_{j+1}$

  (2) There exists a function $\phi \in V_0$, called a scaling function, such that the family $\{\phi(x-k), k \in \mathbb{Z}\}$ is an orthonormal basis of V_0.

  $\Rightarrow \{\phi_{jk}(x) \equiv 2^{j/2}\phi(2^j x - k), k \in \mathbb{Z}\}$ = orthonormal basis of V_j

- Define the spaces W_j by

$$V_j \oplus W_j = V_{j+1}$$

  - V_j = approximation space at resolution 2^j (at level j)
  - W_j = additional details 2^j to 2^{j+1} (called wavelet spaces)

The discrete WT (DWT)

$$\Rightarrow\; L^2(\mathbb{R}) = \bigoplus_{j \in \mathbb{Z}} W_j$$

$$= V_{j_o} \oplus \left(\bigoplus_{j=j_o}^{\infty} W_j \right) \qquad (j_o = \text{lowest resolution level})$$

- Main result :
  $\exists$ function ψ, explicitly computable from ϕ, such that

$$\{\psi_{jk}(x) \equiv 2^{j/2}\psi(2^j x - k), j \in \mathbb{Z}\} \;=\; \text{orthonormal basis of } W_j$$

$$\{\psi_{jk}(x) \equiv 2^{j/2}\psi(2^j x - k), j, k \in \mathbb{Z}\} \;=\; \text{orthonormal basis of } L^2(\mathbb{R})$$

  $\Rightarrow$ orthonormal wavelets

- Examples : Haar wavelets, B-splines, Daubechies wavelets

  Note: B-spline wavelets of order $\geqslant 1$ have compact support, but are not orthogonal to their translates. By orthogonalizing them, one loses compactness of support.

Construction of the mother wavelet

- From $V_0 \subset V_1$, get two-scale or refinement equation

$$\phi(x) = \sqrt{2} \sum_{k=-\infty}^{\infty} h_k \phi(2x-k), \quad h_k = \langle \phi_{1k} | \phi \rangle$$

- Taking Fourier transforms, this gives

$$\widehat{\phi}(2\xi) = h(\xi)\,\widehat{\phi}(\xi), \quad \text{with} \quad h(\xi) = \frac{1}{\sqrt{2}} \sum_{k=-\infty}^{\infty} h_k e^{-ik\xi}$$

- $\Rightarrow$ h is a 2π-periodic function and

$$|h(\xi)|^2 + |h(\xi+\pi)|^2 = 1, \quad h(0) = 1$$

- Iterating the two-scale equation, one gets

$$\widehat{\phi}(\xi) = (2\pi)^{-1/2} \prod_{j=1}^{\infty} h(2^{-j}\xi) \qquad \text{(convergent!)}$$

- Then define $\psi \in W_0 \subset V_1$ by

$$\widehat{\psi}(2\xi) = g(\xi)\,\widehat{\phi}(\xi), \quad \text{with } g \text{ another } 2\pi\text{-periodic function}$$

Construction of the mother wavelet

- By $V_j \oplus W_j = V_{j+1}$ and orthonormality, one gets

$$g(\xi)\,\overline{h(\xi)} + g(\xi+\pi)\,\overline{h(\xi+\pi)} = 0 \tag{1}$$

- Simplest solution: $g(\xi) = e^{i\xi}\,\overline{h(\xi+\pi)}$, which implies

$$|h(\xi)|^2 + |g(\xi)|^2 = 1 \tag{2}$$

(1) and (2) = Smith-Barnwell perfect reconstruction conditions

- The two-scale equation implies

$$h(0) = g(\pi) = 1, \quad h(\pi) = g(0) = 0,$$

i.e. h = low-pass filter, g = high-pass filter

- This gives

$$\psi(x) = \sqrt{2} \sum_{k=-\infty}^{\infty} (-1)^{k-1} h_{-k-1} \phi(2x-k) \qquad \Rightarrow \text{orthonormal basis}$$

- Equivalent solution: $\psi(x) = \sqrt{2}\, \sum_{k=-\infty}^{\infty} (-1)^k h_{-k+1} \phi(2x-k)$

Spline wavelet bases

Simplest example : the Haar basis

- scaling function : $\phi(x) = 1$ for $0 \leqslant x < 1$, and 0 otherwise
- associated wavelet : $\psi_{\rm Haar}(x)$

$$\psi_{\rm Haar}(x) = \begin{cases} 1, & \text{if } 0 \leqslant x < 1/2 \\ -1, & \text{if } 1/2 \leqslant x < 1 \\ 0, & \text{otherwise} \end{cases}$$

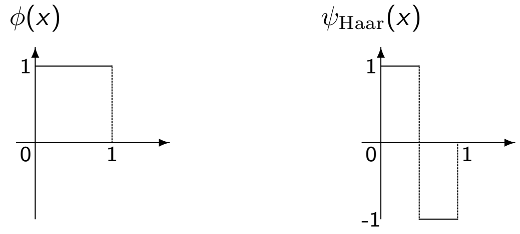

Scaling function $\phi(x)$ Wavelet $\psi_{\rm Haar}(x)$

Spline wavelet bases

Starting from the Haar basis, one builds successive spline wavelet bases of successive order, corresponding to scaling functions

$$\phi_1 = \phi * \phi$$
$$\phi_n = \phi * \phi_{n-1}$$

$$V_0^{(n)} = \{\text{splines of order } n\}$$
$$= \{\text{piecewise polynomial functions of degree } n,\ C^{n-1} \text{ at } k \in \mathbb{Z}\}$$

Spline wavelets of order 1

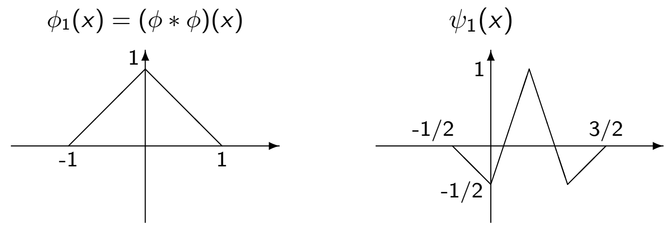

Scaling function $\phi_1(x)$ Wavelet $\psi_1(x)$

Practical implementation of DWT

- Practical formula :
  Sampled signal in V_J $\Rightarrow$ finite representation

$$V_J = V_{j_o} \oplus \left(\bigoplus_{j=j_o}^{J-1} W_j \right), \quad j_o = \text{lowest resolution}$$

- Example with $J = 0$ and $j_o = -6$:

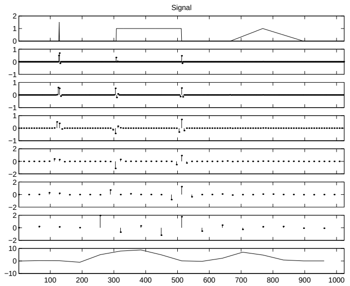

Six level decomposition of a signal on an orthonormal basis of Daubechies d6 wavelets

Discretized CWT vs. DWT

- Question: CWT (discretized) or DWT?
- Answer: Depends on the application
  - CWT for feature detection (no *a priori* choice for a, b) : more flexible, more robust to noise, but only frames in general
  - DWT for large amount of data, data compression : bases, faster, but more rigid (need generalizations)
- Generalizations
  - Biorthogonal wavelets
  - Wavelet packets
  - Continuous wavelet packets (integrated wavelets)
  - Redundant WT (on a rectangular lattice)
  - "Second generation" wavelets (lifting scheme)

Generalization : Biorthogonal wavelet bases

- In CWT, decomposition and reconstruction wavelets may be different (with cross-compatibility conditions)
- Analogue in DWT : biorthogonal bases, starting from two different MRAs $\{V_j\}$, $\{\widetilde{V}_j\}$ with cross-orthogonality conditions between bases $\{\phi_{jk}, k \in \mathbb{Z}\}$ in V_j and $\{\widetilde{\phi}_{jk}, k \in \mathbb{Z}\}$ in $\widetilde{V}_j$
- Wavelet subspaces are defined by
  $W_j \subset V_{j+1}$ and $W_j \perp \widetilde{V}_j$, $\quad \widetilde{W}_j \subset \widetilde{V}_{j+1}$ and $\widetilde{W}_j \perp V_j$
- Choosing bases $\{\psi_{jk}, k \in \mathbb{Z}\}$ in W_j and $\{\widetilde{\psi}_{jk}, k \in \mathbb{Z}\}$ in $\widetilde{W}_j$, one gets

$$\langle \phi_{jk} | \widetilde{\psi}_{j'k'} \rangle = \langle \psi_{jk} | \widetilde{\phi}_{j'k'} \rangle = 0$$
$$\langle \phi_{jk} | \widetilde{\phi}_{j'k'} \rangle = \langle \psi_{jk} | \widetilde{\psi}_{j'k'} \rangle = \delta_{jj'} \delta_{kk'}$$

  $\Longleftrightarrow$ four filters, two low-pass $h, \widetilde{h}$, two high-pass $g, \widetilde{g}$

- This yields
  - more flexibility
  - better control of regularity and decay properties of wavelets
  - easily adaptation to other geometries : wavelets on interval, wavelets on manifolds

Generalization : Wavelet packets

Usual wavelet decomposition scheme:

- At each step, approximation subspace V_j is further decomposed into $V_{j-1} \oplus W_{j-1}$
- And detail subspace W_j is left unchanged
  $\Rightarrow$ unique choice of bases
- This is an asymmetrical subband coding scheme
- Example of a three-level decomposition

<table>
<tr><td colspan="4">V_0</td></tr>
<tr><td colspan="3">V_{-1}</td><td>W_{-1}</td></tr>
<tr><td colspan="2">V_{-2}</td><td>W_{-2}</td><td>W_{-1}</td></tr>
<tr><td>V_{-3}</td><td>W_{-3}</td><td>W_{-2}</td><td>W_{-1}</td></tr>
</table>

Wavelet packet decomposition scheme:

- At each step, both the approximation subspace V_j and the detail subspace W_j are further decomposed

  $\Rightarrow$ large choice of orthonormal bases ("libraries")
- necessity of choosing one particular basis : Best basis algorithm
- Example of wavelet packet three level decomposition, with a particular choice

<table>
<tr><td colspan="8">V_0</td></tr>
<tr><td colspan="4">V_{-1}</td><td colspan="4">W_{-1}</td></tr>
<tr><td colspan="2">V_{-2}</td><td colspan="2">W^0_{-2}</td><td colspan="2">W^1_{-2}</td><td colspan="2">W^2_{-2}</td></tr>
<tr><td>V_{-3}</td><td>W^{00}_{-3}</td><td>W^{01}_{-3}</td><td>W^{02}_{-3}</td><td>W^{11}_{-3}</td><td>W^{12}_{-3}</td><td>W^{21}_{-3}</td><td>W^{22}_{-3}</td></tr>
</table>

- Goal: to build a wavelet system without recourse to Fourier transform, suitable for irregular sampling and arbitrary manifolds
- Observe:
  in a biorthogonal scheme, $\{V_j\}$ does not determine $\{\widetilde{V}_j\}$ uniquely, but freedom of choice is known explicitly (arbitrary trigonometric polynomial)
- Idea: start from given biorthogonal scheme $(h, \widetilde{h}, g, \widetilde{g})$, then tranform it using that freedom into a new one $(h^{(1)}, \widetilde{h}^{(1)}, g^{(1)}, \widetilde{g}^{(1)})$, and so on, by a succession of 'lifting steps'
- Starting point : weaken definition of MRA by imposing only

  (3) for each $j \in \mathbb{Z}$, V_j has a (Riesz) basis $\{\varphi_{j,k}, k \in \mathcal{K}(j)\}$

  with $\mathcal{K}(j)$= general index set, such that $\mathcal{K}(j) \subset \mathcal{K}(j+1)$
  (no dilation invariance $\Rightarrow$ irregular sampling allowed)
- Build dual scale $\{\widetilde{V}_j\}$ with biorthogonal basis

$$\langle \varphi_{j,k} | \widetilde{\varphi}_{j,k'} \rangle = \delta_{kk'}, \; k, k' \in \mathcal{K}(j).$$

- Biorthogonal filters $h, \widetilde{h}$ through refinement equations

$$\varphi_{j,k} = \sum_{l \in \mathcal{K}(j+1)} h_{j,k,l}\, \varphi_{j+1,l}, \quad \text{similarly for } \widetilde{h} \equiv \widetilde{h}_{j,k,l}$$

- Build wavelets in usual way

$$\{\psi_{j,m}, m \in \mathcal{M}(j)\}, \text{ where } \mathcal{M}(j) = \mathcal{K}(j+1) \setminus \mathcal{K}(j)$$

  and dual wavelets, giving biorthogonal basis

$$\langle \psi_{j,m} | \widetilde{\psi}_{j',m'} \rangle = \delta_{jj'} \delta_{mm'}$$

- Refinement equations $\Rightarrow$ filters $g, \widetilde{g}$

$$\psi_{j,m} = \sum_{l \in \mathcal{K}(j+1)} g_{j,m,l}\, \varphi_{j+1,l}\,, \quad \widetilde{\psi}_{j,m} = \sum_{l \in \mathcal{K}(j+1)} g_{j,m,l}\, \widetilde{\varphi}_{j+1,l}\,,$$

  $\Rightarrow$ Four biorthogonal filters $h, \widetilde{h}, g, \widetilde{g}$

- Operator notation: $h_{j,k,l} \Rightarrow$ operator $H_j : \ell^2(\mathcal{K}(j+1)) \to \ell^2(\mathcal{K}(j))$

$$b = H_j a \iff b_k = \sum_{l \in \mathcal{K}(j+1)} h_{j,k,l}\, a_l$$

$$a \equiv (a_l) \in \ell^2(\mathcal{K}(j+1)), b \equiv (b_k) \in \ell^2(\mathcal{K}(j))$$

- $g_{j,m,l} \Rightarrow$ operator $G_j : \ell^2(\mathcal{K}(j+1)) \to \ell^2(\mathcal{M}(j))$
- Similarly for the operators $\widetilde{H}_j, \widetilde{G}_j$
- Conditions for exact reconstruction

$$\begin{pmatrix} \widetilde{H}_j \\ \widetilde{G}_j \end{pmatrix} \begin{pmatrix} H_j^* & G_j^* \end{pmatrix} = \begin{pmatrix} 1 & 0 \\ 0 & 1 \end{pmatrix}$$

$$\begin{pmatrix} H_j^* & G_j^* \end{pmatrix} \begin{pmatrix} \widetilde{H}_j \\ \widetilde{G}_j \end{pmatrix} = 1$$

Lifting scheme

- Freedom in designing a set of filters $\widetilde{H}_j, \widetilde{G}_j$ biorthogonal to H_j, G_j : arbitrary operator $S_j : \ell^2(\mathcal{M}(j)) \to \ell^2(\mathcal{K}(j))$
  (in the simplest case, trigonometric polynomial $s(\xi)$)
- A lifting step:

$$\{H_j, \widetilde{H}_j, G_j, \widetilde{G}_j\} \Longrightarrow \{H_j, \widetilde{H}_j^{(1)}, G_j^{(1)}, \widetilde{G}_j\}$$

$$\text{where } \widetilde{H}_j^{(1)} = \widetilde{H}_j + S_j \widetilde{G}_j, \quad G_j^{(1)} = G_j - S_j^* H_j,$$

- A dual lifting step:

$$\{H_j, \widetilde{H}_j^{(1)}, G_j^{(1)}, \widetilde{G}_j, \} \Longrightarrow \{H_j^{(1)}, \widetilde{H}_j^{(1)}, G_j^{(1)}, \widetilde{G}_j^{(1)}, \}$$

$$\text{where } H_j^{(1)} = H_j + \widetilde{S}_j G_j^{(1)}, \quad \widetilde{G}_j^{(1)} = \widetilde{G}_j - \widetilde{S}_j^* \widetilde{H}_j^{(1)}$$

- $\Longrightarrow$ can get any biorthogonal filter set after finite number of steps, starting from the Lazy wavelet: $H_j = \widetilde{H}_j = E$, $G_j = \widetilde{G}_j = D$, where
  $E : \ell^2(\mathcal{K}(j+1)) \to \ell^2(\mathcal{K}(j))$ and $D : \ell^2(\mathcal{K}(j+1)) \to \ell^2(\mathcal{M}(j))$
  are restriction (subsampling) operators

- Basis $\{f_k\}_{k\in I}$ in Hilbert space $\mathcal{H}$ (not necessarily orthogonal !): every $f \in \mathcal{H}$ can be represented as

$$f = \sum_{k\in I} c_k(f) f_k \tag{3}$$

  with unique coefficients $c_k(f)$
- Frame $\{f_k\}_{k\in I}$ in $\mathcal{H}$: every $f \in \mathcal{H}$ may also be written as in (3), but the coefficients are not necessarily unique (maybe linearly dependent) $\Longrightarrow$ redundancy
- For every frame $\{f_k\}_{k\in I}$, there exists a dual frame $\{\widetilde{f}_k\}_{k\in I}$ such that

$$f = \sum_{k\in I} \langle f, f_k\rangle \widetilde{f}_k = \sum_{k\in I} \langle f, \widetilde{f}_k\rangle f_k, \ \forall f \in \mathcal{H}.$$

  Problems : convergence? good appproximation by truncation?
- Question: What is better: wavelet bases or frames?

SOME GENERAL CONSIDERATIONS ON BASES AND FRAMES

- For each $j \in \mathbb{Z}$, $V_{j+1} = V_j \bigoplus W_j$
  Choose bases $\Phi^j = (\phi_{jk})_k$ in V_j, $\Psi^j = (\psi_{jk})_k$ in W_j (row vectors)
- Any $f^j = \sum_{k=1}^{n_j} f_k^j \phi_{jk} \in V_j$ and $g^j = \sum_{k=1}^{m_j} g_k^j \psi_{jk} \in W_j$ can be written as

$$f^j = \Phi^j \mathbf{f}^j, \quad g^j = \Psi^j \mathbf{g}^j, \quad \text{with } \mathbf{f}^j = (f_k^j)_j,\ \mathbf{g}^j = (g_k^j)_j \text{ column vectors}$$

- Since $V_{j-1}, W_{j-1}$are subspaces of $V_j = V_{j-1} \oplus W_{j-1}$, we may write

$$\Phi^{j-1} = \Phi^j P^j \text{ and } \Psi^{j-1} = \Phi^j Q^j \qquad (*)$$

- Given f^j, $\exists !\ f^{j-1} \in V_{j-1}$, $g^{j-1} \in W_{j-1}$ such that

$$f^j = f^{j-1} + g^{j-1} \quad \Longleftrightarrow \quad \Phi^j \mathbf{f}^j = \Phi^{j-1}\mathbf{f}^{j-1} + \Psi^{j-1}\mathbf{g}^{j-1}$$

- So, using $(*)$, we get $\mathbf{f}^j = \underbrace{(P^j \ \ Q^j)}_{= M_j \,:\, \text{two-scale matrix}} \begin{pmatrix} \mathbf{f}^{j-1} \\ \mathbf{g}^{j-1} \end{pmatrix}$
- The two-scale matrix has to be inverted for some applications : sparse, orthogonal?

What is desirable from a wavelet basis/frame?

- continuity, smoothness (if we want to approximate smooth data)
- orthogonality
- local support
- Riesz stability (for nonorthogonal bases)
- vanishing moments
- for spherical wavelets: absence of distortions around pole(s)
- ...

Desirable properties : Why orthogonality ?

- In some applications (like compression, denoising) one needs to invert the two-scale matrix M_j.
  Thus, orthogonality $\Longrightarrow$ fast algorithms
- However, orthogonality is often difficult to achieve
  (for example, on $\mathbb{R}$, there is no symmetric orthogonal wavelet ψ with compact support)
- In many situations, the orthogonality requirement is relaxed to semi-orthogonality or biorthogonality

Desirable properties : Why orthogonality ?

- Let $L^2(\mathbb{R}) = \ldots \oplus W^{-1} \oplus W^0 \oplus W^1 \oplus W^2 \oplus \ldots$

  $$\mathcal{B}_j = \{\psi_{j,k},\ k \in \mathbb{Z}\} \text{ basis in } W^j,\ \mathcal{B} = \{\psi_{j,k},\ j,k \in \mathbb{Z}\} \text{ basis in } L^2(\mathbb{R})$$

- Orthogonal wavelet basis $\{\psi_{j,k},\ j,k \in \mathbb{Z}\}$:

  $$\langle \psi_{j,k}, \psi_{j',k'} \rangle = \delta_{j,j'}\delta_{k,k'}$$

  One has

  $$f = \sum_{j,k\in\mathbb{Z}} \langle f, \psi_{j,k} \rangle \psi_{j,k},\ \forall f \in L^2(\mathbb{R})$$

- Semi-orthogonal wavelet basis $\mathcal{B}$: $\langle \psi_{j,k}, \psi_{j',k'} \rangle = \delta_{j,j'}\, c(k,k')$
- Biorthogonal wavelet bases generated by $\psi, \widetilde{\psi}$:

  $$\langle \psi_{j,k}, \widetilde{\psi_{j',k'}} \rangle = \delta_{j,j'}\delta_{k,k'}$$

  $$f = \sum_{j,k\in\mathbb{Z}} \langle f, \widetilde{\psi_{j,k}} \rangle \psi_{j,k} = \sum_{j,k\in\mathbb{Z}} \langle f, \psi_{j,k} \rangle \widetilde{\psi_{j,k}}, \quad \forall f \in L^2(\mathbb{R})$$

Desirable properties : Why local support ?

- Local support implies that the two-scale matrix M_j is sparse (crucial for large amount of data)

  Recall: $\mathbf{f^j} = (P^j\ Q^j) \begin{pmatrix} \mathbf{f^{j-1}} \\ \mathbf{g^{j-1}} \end{pmatrix}$, $M_j = (P^j\ Q^j)$
- Local support prevents spread of "tails"

  Example: Using a spherical harmonics kernel, localized, but not locally supported, leads to "ripples" when approximating data

Desirable properties : Why local support ?

A spherical harmonics kernel in spherical coordinates and on the sphere : localized, but not locally supported

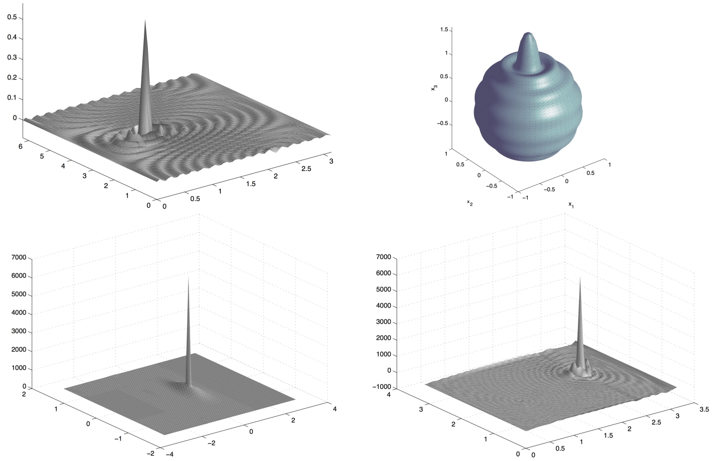

Initial data set and its approximation at level 6

Desirable properties : Why Riesz stability ?

- Let $J =$ countable, $\mathcal{H}$ Hilbert space. Then the basis $\{f_k\}_{k\in J} \subset \mathcal{H}$ satisfies the Riesz stability conditions if $\exists\ A > 0, B < \infty$ such that

$$A \sum_{k\in J} |c_k|^2 \leqslant \| \sum_{k\in J} c_k f_k \|^2 \leqslant B \sum_{k\in J} |c_k|^2 \quad \forall c = \{c_k\} \in l^2(J).$$

- Meaning of stability: Let $g = \sum_{k\in J} d_k f_k,\ g^* = \sum_{k\in J} d^*_k f_k \in \mathcal{H}$
  Then the Riesz stability requirement is equivalent to the inequalities

$$\|g - g^*\| \leqslant B^{1/2} \|d - d^*\|_{l^2(J)} \text{ and } \|d - d^*\|_{l^2(J)} \leqslant A^{-1/2} \|g - g^*\|,$$

  where $d = \{d_k\}_{k\in J},\ d^* = \{d^*_k\}_{k\in J}$
  - Small perturbation on coefficients $d_k \Rightarrow$ the function g can be reconstructed with small error
  - Small perturbation of $g \Rightarrow$ small perturbation of the coefficients d_k
- Moreover, if there exists a Riesz stable basis, then there exists a biorthogonal basis $\{\widetilde{f_k}\}_{k\in J} \subset \mathcal{H}$ such that

$$\langle f_i, \widetilde{f_j} \rangle = \delta_{ij} \text{ and } f = \sum_{k\in J} \langle f, \widetilde{f_k} \rangle f_k = \sum_{k\in J} \langle f, f_k \rangle \widetilde{f_k}, \quad \forall f \in \mathcal{H}.$$

Desirable properties : Why vanishing moments ?

- Vanishing moments:

$$\int_{\mathbb{R}} x^n \widetilde{\psi}(x)\, dx = 0, \text{ for } n = 0, 1, \ldots, N$$

  $\Longrightarrow \widetilde{\psi}$ blind to polynomials of degree $\leqslant N$
  (smooth part of the signal)

  $\Longrightarrow$ good for detections of singularities

- For DWT:

$$f = \sum_{j,k} d_{j,k} \psi_{j,k}, \qquad d_{j,k} = \langle f, \widetilde{\psi}_{j,k} \rangle$$

  Important result: $|d_{j,k}|$ is large only in the region where f is less smooth (unlike Fourier series, where a discontinuity of f ruins the decrease of *all* Fourier coefficients)

WAVELET ANALYSIS OF 2-D IMAGES

- Geometric transformations in the plane $\mathbb{R}^2$:

  (i) translation by $\vec{b} \in \mathbb{R}^2 : \vec{x} \mapsto \vec{x}' = \vec{x} + \vec{b}$
  (ii) dilation by a factor $a > 0 : \vec{x} \mapsto \vec{x}' = a\vec{x}$
  (iii) rotation by an angle $\theta : \vec{x} \mapsto \vec{x}' = r_\theta(\vec{x})$

$$r_\theta \equiv \begin{pmatrix} \cos\theta & -\sin\theta \\ \sin\theta & \cos\theta \end{pmatrix}, \ 0 \leqslant \theta < 2\pi, \ \text{rotation matrix}$$

- Action on finite energy signals

$$\left[U(\vec{b}, a, \theta)s\right](\vec{x}) \equiv s_{\vec{b},a,\theta}(\vec{x}) = a^{-1} s(a^{-1}\, r_{-\theta}(\vec{x} - \vec{b}))$$

- Basic formulas for CWT :

$$\begin{aligned} S(\vec{b}, a, \theta) &= \langle \psi_{\vec{b},a,\theta} | s \rangle \\ &= a^{-1} \int_{\mathbb{R}^2} \overline{\psi(a^{-1}\, r_{-\theta}(\vec{x} - \vec{b}))}\, s(\vec{x})\, d^2\vec{x} \\ &= a \int_{\mathbb{R}^2} e^{i\vec{b}\cdot\vec{k}}\, \overline{\widehat{\psi}(a r_{-\theta}(\vec{k}))}\, \widehat{s}(\vec{k})\, d^2\vec{k} \end{aligned}$$

- Admissibility of wavelet ψ :

$$c_\psi \equiv (2\pi)^2 \int_{\mathbb{R}^2} \frac{|\widehat{\psi}(\vec{k})|^2}{|\vec{k}|^2}\, d^2\vec{k} < \infty$$

- Necessary condition :

$$\widehat{\psi}(\vec{0}) = 0 \iff \int_{\mathbb{R}^2} \psi(\vec{x})\, d^2\vec{x} = 0.$$

- Note : all formulas almost identical in 1-D and in 2-D !

- Dilation + translation = affine transformation of the line

$$y = (b, a)x \equiv ay + b, \quad a \neq 0, \ b \in \mathbb{R}, \ x \in \mathbb{R}$$

- Composition rule : $(b, a)(b', a') = (b + ab', aa')$
  $\Rightarrow \{(b, a)\} \equiv G_{\mathrm{aff}} \simeq \mathbb{R}^2_* =$ affine group
- Action of (b, a) on the signal : $\psi \mapsto U(b, a)\psi$

$$(U(b, a)\psi)(x) = |a|^{-1/2}\psi\left(\frac{x - b}{a}\right) \qquad (*)$$

  and U = unitary irreducible representation of G_{aff} in $L^2(\mathbb{R})$
- U is square integrable

$$\psi \text{ admissible} \iff \iint_{G_{\mathrm{aff}}} |\langle U(b, a)\psi|\psi\rangle|^2\, \frac{db\, da}{a^2} < \infty$$

- Note : Restricting to $a > 0$, one gets the connected affine group G^+_{aff} (or $ax + b$ group) and $(*)$ is a UIR of it in $L^2(\mathbb{R}^+)$

- Dilations + translations + rotations
  = similitude group of the plane : $\mathrm{SIM}(2) = \mathbb{R}^2 \rtimes (\mathbb{R}^+_* \times \mathrm{SO}(2))$

$$\vec{y} = (\vec{b}, a, \theta)\vec{x} \equiv a r_\theta \vec{x} + \vec{b},$$

- Action on finite energy signals

$$\left[U(\vec{b}, a, \theta)s\right](\vec{x}) = a^{-1} s(a^{-1}\, r_{-\theta}(\vec{x} - \vec{b}))$$

  and U = unitary irreducible representation of SIM(2) in $L^2(\mathbb{R}^2)$
- U is square integrable

$$\psi \text{ admissible} \iff \iiint_{\mathrm{SIM}(2)} \left|\langle U(\vec{b}, a, \theta)\psi|\psi\rangle\right|^2\, d^2\vec{b}\, \frac{da}{a^3}\, d\theta < \infty$$

Interpretation of CWT : exactly as in 1-D

- localization properties of ψ + convolution with zero mean function $\Rightarrow$ local filtering in $\vec{b}, a, \theta$
- support properties of $\psi \Rightarrow$ analysis with constant relative bandwidth: $\Delta k/k =$ const, $k = |\vec{k}|$

  $\Rightarrow$ CWT = mathematical directional microscope
  (optics ψ, global magnification $1/a$, orientation tuning parameter θ)

  $\Rightarrow$ CWT = detector and analyzer of singularities
  (edges, contours, corners, ...)

- Energy conservation

$$c_\psi^{-1} \iiint_{\mathrm{SIM}(2)} |S(\vec{b}, a, \theta)|^2 \, d^2\vec{b} \, \frac{da}{a^3} \, d\theta = \int_{\mathbb{R}^2} |s(\vec{x})|^2 \, d^2\vec{x}$$

  i.e., isometry from space of signals $L^2(\mathbb{R}^2)$ onto closed subspace of $L^2(\mathrm{SIM}(2))$ = space of wavelet transforms

- Reconstruction formula
  Inversion of CWT by adjoint map :

$$s(\vec{x}) = c_\psi^{-1} \iiint_{\mathrm{SIM}(2)} \psi_{\vec{b},a,\theta}(\vec{x}) \, S(\vec{b}, a, \theta) \, d^2\vec{b} \, \frac{da}{a^3} \, d\theta$$

  i.e., decomposition of the signal in terms of the analyzing wavelets $\psi_{\vec{b},a,\theta}$, with coefficients $S(\vec{b}, a, \theta)$

- Reproduction property (reproducing kernel)

$$S(\vec{b}', a', \theta') = c_\psi^{-1} \iiint_{\mathrm{SIM}(2)} \langle \psi_{\vec{b}',a',\theta'} | \psi_{\vec{b},a,\theta} \rangle \, S(\vec{b}, a, \theta) \, d^2\vec{b} \, \frac{da}{a^3} \, d\theta$$

- WT is covariant under translations, dilations and rotations

(i) *Isotropic wavelets*

- Pointwise analysis
- Directions irrelevant

$\Rightarrow$ rotation invariant wavelet

Examples :

- 2-D Mexican hat wavelet

$$\psi_H(\vec{x}) = (2 - |\vec{x}|^2) \exp(-\tfrac{1}{2}|\vec{x}|^2)$$

$$\widehat{\psi}_H(\vec{k}) = |\vec{k}|^2 \exp(-\tfrac{1}{2}|\vec{k}|^2)$$

- Difference-of-Gaussians or DOG wavelet

$$\psi_D(\vec{x}) = \frac{1}{2\alpha^2} \exp(-\frac{1}{2\alpha^2}|\vec{x}|^2) - \exp(-\tfrac{1}{2}|\vec{x}|^2) \qquad (0 < \alpha < 1)$$

An isotropic wavelet: The 2-D Mexican hat wavelet

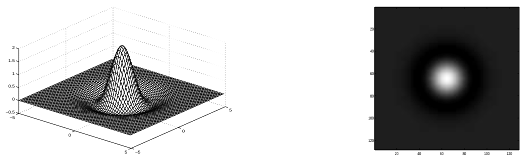

in position space

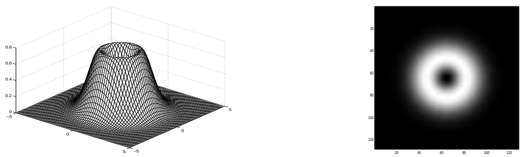

in spatial frequency space

(ii) *Directional wavelets*

- Detection of directional features
- Directional filtering

$\Rightarrow$ direction sensitive wavelet

Example :
directional wavelet $\Leftrightarrow$ num supp $\widehat{\psi} \subset$ convex cone, apex at 0

- 2-D Morlet wavelet

$$\psi_M(\vec{x}) = \exp(i\vec{k}_o \cdot \vec{x}) \, \exp(-\tfrac{1}{2}|\vec{x}|^2) + \text{corr.}$$

$$\widehat{\psi}_M(\vec{k}) = \exp(-\tfrac{1}{2}|\vec{k} - \vec{k}_o|^2) + \text{corr.}$$

- Conical wavelet, with support in convex cone

$$C(-\alpha, \alpha) \equiv \{\vec{k} \in \mathbb{R}^2 \,|\, -\alpha \leqslant \arg \vec{k} \leqslant \alpha, \; \alpha < \pi/2\}$$

$$\widehat{\psi}_C(\vec{k}) = \begin{cases} (\vec{k} \cdot \vec{e}_{-\tilde{\alpha}})^m (\vec{k} \cdot \vec{e}_{\tilde{\alpha}})^m \, e^{-\frac{1}{2}k_x^2}, & \vec{k} \in C(-\alpha, \alpha) \\ 0, \text{ otherwise} \end{cases}$$

- A directional wavelet : The 2-D Morlet wavelet

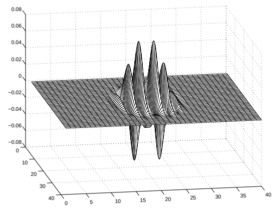

in position space

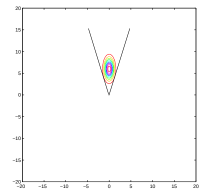

in spatial frequency space

- A very directional wavelet : The Gaussian conical wavelet (in spatial frequency space)

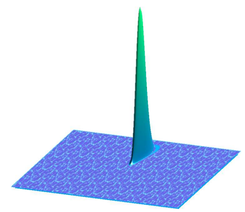

(a) 2-D frames:
same definition as in 1-D, similar results (Mexican hat, Morlet wavelet, ...give good, nontight frames)

(b) 2-D ridges:
Caution: several possible definitions !!

Useful choice, in terms of energy density of the CWT :

$$\mathrm{E}[s](\vec{b}, a) \equiv |S(\vec{b}, a)|^2 \quad \text{(in isotropic case)}$$

Ridges = lines of local maxima of $\mathrm{E}[s](\vec{b}, a)$
Skeleton = set of all ridges

- More precisely, a (vertical) ridge $\mathcal{R}$ is a 3-D curve $(\vec{r}(a), a)$ such that, for each scale $a \in \mathbb{R}^+$, $\mathrm{E}[s](\vec{r}(a), a)$ is locally maximum in space and r is a continuous function of scale
- As in 1-D, the restriction of the CWT to its skeleton characterizes the signal completely.

- Characteristic features of a ridge:
  - Amplitude of the ridge

$$\mathcal{A}_{\mathcal{R}} = \lim_{a \to 0} \mathrm{E}[s](\vec{r}(a), a)$$

  - Slope of $\mathrm{E}[s]$ on the ridge

$$\mathcal{S}_{\mathcal{R}} = \lim_{a \to 0} \frac{d \ln \mathrm{E}[s](\vec{r}(a), a)}{d \ln a}$$

  - Energy of the ridge

$$\mathcal{E}_{\mathcal{R}} = \int_0^{a_{\max}} \mathrm{E}[s](\vec{r}(a), a) \, \frac{da}{a^3}$$

- An example of 2-D vertical ridges

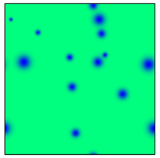

Simulated bright points on the Sun

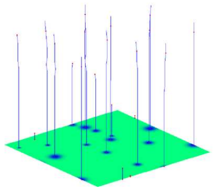

Corresponding vertical ridges

- Image denoising
  removal of noise in images using directional wavelets
- Contour detection, character recognition
  detection of edges, contours, corners ...
- Object detection and recognition in noisy images
  automatic target recognition (ATR), application to infrared radar imagery, using both position and scale-angle features
- Image retrieval
  recognition of a particular image in a large data basis, characterization of images by particular features
- Medical imaging
  Magnetic resonance imaging (MRI), contrast enhancement, segmentation
- Watermarking of images
  adding a robust, but invisible, signature in images (e.g. with directional wavelets)

- Astronomy and astrophysics
  structure of the Universe, cosmic microwave background (CMB) radiation, feature detection in images of the Sun, detection of gamma-ray sources in the Universe
- Geophysics
  geology: fault detection, seismology, climatology
- Fluid dynamics
  detection of coherent structures in turbulent fluids, measurement of a velocity field, disentangling of an underwater acoustic wave train

- Fractals and the thermodynamical formalism
  analysis of 2-D fractals by the WTMM method (diffusion limited aggregates, arborescent growth phenomena, fractal surfaces, clouds,...) :
  determination of fractal dimension, unraveling of universal laws, shape recognition and classification of patterns
- Texture analysis
  classification of textures, "Shape from texture" problem
- Detection of symmetries in 2-D patterns
  detection of discrete inflation (rotation + dilation) symmetries, quasicrystals (mathematical and genuine), quasiperiodic point sets

Noise removal in images

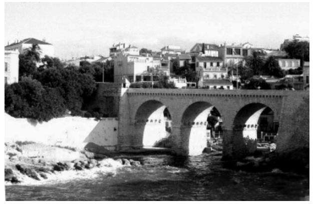

Clear image

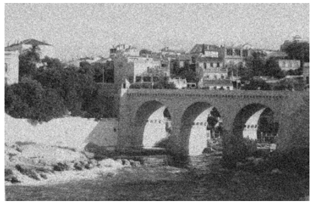

Noisy image

Reconstructed, denoised image

Contour detection

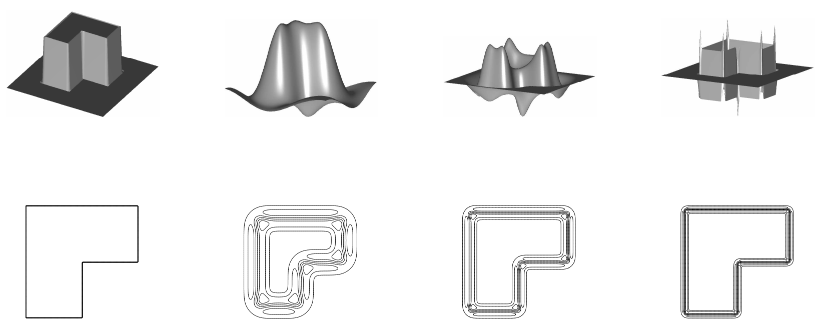

The signal $a = 8$ $a = 4$ $a = 2$

Example of character recognition

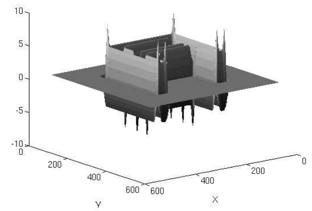

1 1
-1 -1

-1 -1
-1 -1

1 1 1 1

Detecting the contour of the letter A with the radial Mexican hat:
The CWT and its coding by the signs of the respective corners

Solar physics : Disentangling bright points from cosmic hits on solar images

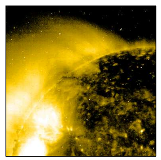

Top-left quadrant of a 284 Å wavelength EIT/SoHO image

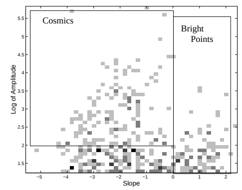

Slope-amplitude histogram

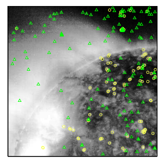

Selected cosmics (triangles) and bright points (circles)

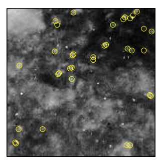

Bright points selection

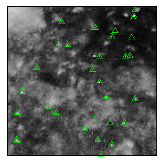

Cosmics selection

A closer look on a small on-disk region of the Sun

Directional filtering with a conical wavelet

Signal — CWT — CWT after thresholding

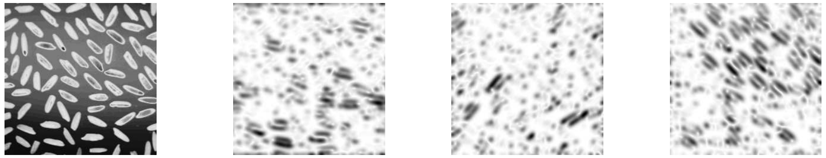

The original image, representing bacteria — Filtering at -10° — The same at 45° — The same at 135°

Measuring the velocity field in a turbulent fluid (with Morlet wavelet)

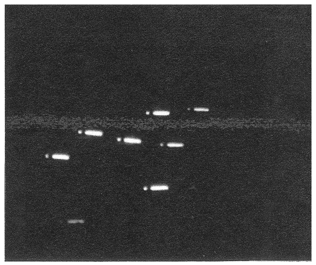

The dot-bar signature of tracers in the fluid

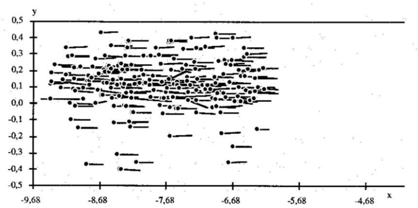

A quasi-laminar flow

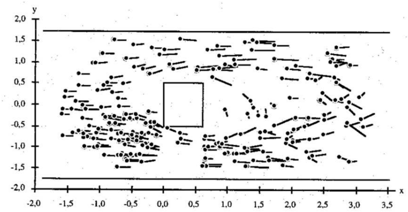

A turbulent flow around an obstacle

- Choose dilation matrix D : 2×2 regular matrix such that
  - (a) $D\mathbb{Z}^2 \subset \mathbb{Z}^2$ ($\Leftrightarrow D$ has integer entries)
  - (b) $\lambda \in \sigma(D) \Rightarrow |\lambda| > 1$
- A multiresolution analysis of $L^2(\mathbb{R}^2)$ is an increasing sequence of closed subspaces $\mathbf{V}_j \subset L^2(\mathbb{R}^2)$:

$$\ldots \subset \mathbf{V}_{-2} \subset \mathbf{V}_{-1} \subset \mathbf{V}_0 \subset \mathbf{V}_1 \subset \mathbf{V}_2 \subset \ldots$$

such that

- (1) $\bigcap_{j\in\mathbb{Z}} \mathbf{V}_j = \{0\}$, $\overline{\bigcup_{j\in\mathbb{Z}} \mathbf{V}_j} = L^2(\mathbb{R}^2)$ (exhaustion)
- (2) $f(\cdot) \in \mathbf{V}_j \iff f(D\,\cdot) \in \mathbf{V}_{j+1}$ (no privileged scale)
- (3) $\exists\, \Phi \in L^2(\mathbb{R}^2)$ s.t. $\{\Phi(\cdot - \mathbf{k}),\ \mathbf{k} \in \mathbb{Z}^2\}$ is an orthonormal basis of $\mathbf{V}_0$ (scaling function)

$$\Longrightarrow \{\Phi_{j,\mathbf{k}}(\cdot) = |\det D|^{j/2}\Phi(D^j \cdot - \mathbf{k}),\ \mathbf{k} \in \mathbb{Z}^2\} \text{ orthonormal basis of } \mathbf{V}_j$$

Define $\mathbf{W}_j$: $\mathbf{V}_{j+1} = \mathbf{V}_j \oplus \mathbf{W}_j$.

- 2-D wavelets: functions in $\mathbf{W}_0$.
- Theorem [Meyer]: There exist $q = |\det D| - 1$ wavelets

$$^1\Psi, ^2\Psi, \ldots, ^q\Psi \in \mathbf{V}_1$$

that generate an orthonormal basis of $\mathbf{W}_0$. These functions can be constructed explicitly from the scaling function Φ.

$$\Longrightarrow \{^\nu\Psi_{j,\mathbf{k}}(\cdot) = |\det D|^{j/2} \cdot {}^\nu\Psi(D^j \cdot - \mathbf{k}),\ \nu = 1, \ldots, q,\ \mathbf{k} \in \mathbb{Z}^2\}$$
$$= \text{orthonormal basis of } \mathbf{W}_j$$

$$\{^\nu\Psi_{j,\mathbf{k}},\ \nu = 1, \ldots, q,\ \mathbf{k} \in \mathbb{Z}^2,\ j \in \mathbb{Z}\} = \text{orthonormal basis of } L^2(\mathbb{R}^2)$$

- Particular case: tensor product wavelets

  Take
  $$D = \begin{pmatrix} 2 & 0 \\ 0 & 2 \end{pmatrix},$$

  Let $\{V_j, j \in \mathbb{Z}\}$ be a 1-D MRA in $L^2(\mathbb{R})$. Then the 2-D scaling function $\Phi(\mathbf{x}) = \phi(x)\phi(y)$ generates a MRA of $L^2(\mathbb{R}^2)$ and

  $$\begin{aligned} \mathbf{V}_{j+1} &= V_{j+1} \otimes V_{j+1} = (V_j \oplus W_j) \otimes (V_j \oplus W_j) \\ &= (V_j \otimes V_j) \oplus [(W_j \otimes V_j) \oplus (V_j \otimes W_j) \oplus (W_j \otimes W_j)] \\ &= \mathbf{V}_j \oplus \mathbf{W}_j. \end{aligned}$$

  Thus $\mathbf{W}_j$ consists of three pieces, with the following orthonormal bases :

  $$\begin{aligned} &\{\psi_{j,k_1}(x)\phi_{j,k_2}(y),\ (k_1,k_2) \in \mathbb{Z}^2\} \text{ o.n.b. for } W_j \otimes V_j, \\ &\{\phi_{j,k_1}(x)\psi_{j,k_2}(y),\ (k_1,k_2) \in \mathbb{Z}^2\} \text{ o.n.b. for } V_j \otimes W_j, \\ &\{\psi_{j,k_1}(x)\psi_{j,k_2}(y),\ (k_1,k_2) \in \mathbb{Z}^2\} \text{ o.n.b. for } W_j \otimes W_j. \end{aligned}$$

$\Rightarrow$ one scaling function : $\Phi(x,y) = \phi(x)\phi(y)$

and three wavelets :

$$\begin{aligned} {}^h\Psi(x,y) &= \phi(x)\psi(y) \\ {}^v\Psi(x,y) &= \psi(x)\phi(y) \\ {}^d\Psi(x,y) &= \psi(x)\psi(y) \end{aligned}$$

Then

$\{{}^\lambda\Psi_{j,\mathbf{k}},\ \mathbf{k} = (k_1,k_2) \in \mathbb{Z}^2,\ \lambda = h,v,d\}$ is an o.n.b. for $\mathbf{W}_j$

$\{{}^\lambda\Psi_{j,\mathbf{k}},\ j \in \mathbb{Z},\ \mathbf{k} \in \mathbb{Z}^2,\ \lambda = h,v,d\}$ is an o.n.b. for

$$\overline{\bigoplus_{j\in\mathbb{Z}} \mathbf{W}_j} = L^2(\mathbb{R}^2)$$

ϕ, ψ have compact support $\Longrightarrow$ $\Phi, {}^\lambda\Psi$ have compact support

Typical 3-level decomposition of an image

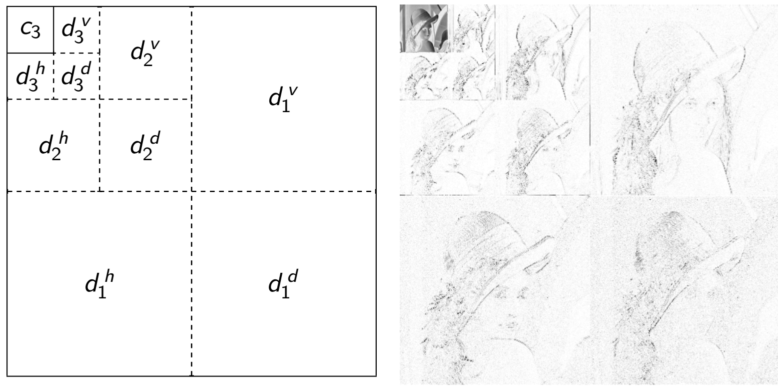

EXTENDING THE CWT TO THE TWO-SPHERE

Extending the CWT to curved manifolds

- Many situations in physics yield data on non-flat manifolds:
  - sphere : geophysics, cosmology (CMB), statistics, ...
  - two-sheeted hyperboloid : cosmology (an open expanding model of the universe), optics (catadioptric image processing, where a sensor overlooks a hyperbolic mirror)
  - paraboloid : optics (catadioptric image processing)

$\Rightarrow$ suitable analysis tools?

- Possible solution: extend the continuous wavelet transform
  - easy translation of the wavelet, by an isometry of the manifold, i.e., an element of SO(3), SO(1,2)...
  - local transform, with locality controlled by a dilation (to be defined!)
  - in practice, usual CWT works with discrete frames

    $\Rightarrow$ need discrete wavelet frames on manifold

Wavelet transforms on the 2-sphere

- Do we have suitable analysis tools for signals living on the 2-sphere?
  Unit sphere : $\mathbb{S}^2 = \{\mathbf{x} \in \mathbb{R}^3,\ \|\mathbf{x}\| = 1\}$
- Fourier transform is standard, but cumbersome : expansion in spherical harmonics !

  $\{Y_l^m(\theta,\varphi)\}$ o.n. basis on $L^2(\mathbb{S}^2)$, so that, $\forall\, f \in L^2(\mathbb{S}^2, d\mu(\omega))$,

$$\begin{aligned} f(\omega) &= \sum_{l\in\mathbb{N}} \sum_{|m|\leqslant l} \widehat{f}(l,m)\, Y_l^m(\omega), \\ \widehat{f}(l,m) &= \langle Y_l^m | f\rangle = \int_{\mathbb{S}^2} \overline{Y_l^m(\omega)}\, f(\omega)\, d\mu(\omega) \end{aligned}$$

  where $\omega = (\theta,\varphi) \in \mathbb{S}^2,\ \theta \in [0,\pi],\ \varphi \in [0,2\pi),\ d\mu(\omega) = \sin\theta\, d\theta\, d\varphi$
- Problem : global analysis, Y_l^m not localized at all on the sphere!
  Note: there exist localized combinations (spherical harmonics kernels, as seen before)

The CWT on the sphere

- How to define a CWT on the sphere?
  Translations $\Rightarrow$ rotations from SO(3)
  Dilations ? the sphere is compact !
- Can one use the existing results from 2-D (frames, directional wavelets, etc.) ?
- Successive approaches
  - W. Freeden & U. Windheuser (1995, 1996) (via spherical harmonics)
  - M. Holschneider (1996)
  - S. Dahlke & P. Maass (1996)
  - J-P. Antoine & P. Vandergheynst (1998)
- The continuous wavelet transform (CWT) has many advantages :
  - locality controlled by a dilation (to be defined!)
  - easy translation of the wavelet, by a rotation from SO(3)
  - reasonably fast algorithms
  - possibility of constructing spherical frames

The DWT on the sphere

MRA on $L^2(\mathbb{S}^2)$

- A multiresolution analysis of $L^2(\mathbb{S}^2)$ is an increasing sequence of closed subspaces $\{\mathcal{V}^j,\ j \geqslant 0\}$

$$\mathcal{V}^0 \subset \mathcal{V}^1 \subset \mathcal{V}^2 \subset \ldots \subset L^2(\mathbb{S}^2)$$

  such that
  - $\bigcup_{j=0}^{\infty} \mathcal{V}^j$ is dense in $L^2(\mathbb{S}^2)$
  - $\exists$ index sets $\mathcal{K}_j \subseteq \mathcal{K}_{j+1}$ s.t., $\forall\, j, \mathcal{V}^j$ has a Riesz basis $\{\varphi_v^j,\ v \in \mathcal{K}_j\}$. More precisely, there exist constants $0 < A \leqslant B < \infty$, independent of the level j, such that

$$A\, 2^{-j} \left\| \left\{ c_v^j \right\}_{v\in\mathcal{K}_j} \right\|_{l_2(\mathcal{K}_j)} \leqslant \left\| \sum_{v\in\mathcal{K}^j} c_v^j \varphi_v^j \right\|_{L^2(\mathbb{S}^2)} \leqslant B\, 2^{-j} \left\| \left\{ c_v^j \right\}_{v\in\mathcal{K}^j} \right\|_{l_2(\mathcal{K}_j)}$$

    (we do not require that φ_v^j = translations/dilations of the same function φ: too difficult for spherical wavelet frames/bases)
- Define the wavelet spaces $\mathcal{W}^j$ as $\mathcal{W}^j = \mathcal{V}^{j+1} \ominus \mathcal{V}^j$ and then construct a basis in each $\mathcal{W}^j$

Main approaches in literature

- Via spherical harmonics kernels :
  - D. Potts, G. Steidl, M. Tasche (1996) spherical frames

    no distortion (no pole has a privileged role), preserves smoothness, but frame is not locally supported
  - F. Narcowich & J.D. Ward (1996)
  - W. Freeden & U. Windheuser (1997)
  - T. Bülow (2002) : diffusion, heat equation on the sphere
  - W. Freeden & M. Schreiner (1997, 2006)

    wavelets locally supported, but they are defined as infinite convolutions of kernels of spherical harmonics
  - W. Freeden & M. Schreiner (2007)

    wavelets are locally supported, but the MRA is truncated at $j = N$

$$\{0\} \subset \mathcal{V}^0 \subset \mathcal{V}^1 \subset \ldots \subset \mathcal{V}^{N-1} \subset \mathcal{V}^N \subset L^2(\mathbb{S}^2).$$

  - H. Mhaskar, J. Prestin (2006) (spherical) polynomial frames
- Via polar coordinates $(\theta, \varphi) \in [0, \pi] \times [0, 2\pi] \to \mathbb{S}^2$

For localization : kernels of spherical harmonics, localized, but not locally supported!

- Analogy in 1-D: Dirichlet kernel : $D_N(x) = \dfrac{1}{2\pi} \displaystyle\sum_{k=-N}^{N} e^{ikx}$

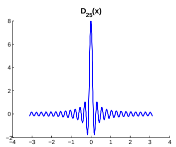

- Spherical harmonics kernel at level j : $\Phi^j = \dfrac{1}{2^j} \displaystyle\sum_{l=0}^{2^j-1} \sum_{m=-l}^{l} (2l+1) Y_l^m$

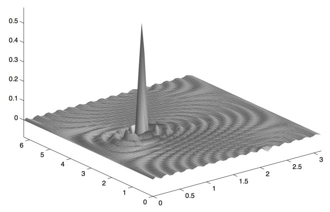

in polar coordinates

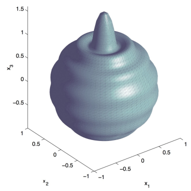

on the sphere

- Via radial projection from a convex polyhedron Γ + weighted scalar product on $\mathbb{S}^2$: D. Roșca (2005, 2006, 2007)

  In this way one gets
  - Piecewise constant wavelets on spherical triangulations
  - Piecewise linear wavelets on triangulations of $\mathbb{R}^2 \rightsquigarrow$ Piecewise rational semi-orthogonal wavelets on $\mathbb{S}^2$: continuous
  - Γ = cube + wavelets on an interval $\rightsquigarrow$ Haar wavelets on $\mathbb{S}^2$

  Properties : Riesz stability, local support ($\Longrightarrow$ sparse matrices), no distortion around the poles, easy implementation, possible extension to sphere-like surfaces (closed surfaces), but no smoothness
- Other methods : direct calculations on the sphere, $\mathbb{S}^2$ MRA on spherical meshes, using lifting scheme (P. Schröder et W. Sweldens, 1995)
- Important observation : no construction mentioned so far yields simultaneously continuity & local support & orthogonality of the wavelet bases (OK for every choice of 2 conditions + no distortions around poles)
- DWT on the sphere via stereographic projection:

  J-P. Antoine & D. Roșca (2007)

- Origin of the spherical CWT : affine transformations on $\mathbb{S}^2$
  - motion = rotation $\varrho \in SO(3)$
  - dilation by scale factor $a \in \mathbb{R}_+^*$: how to define it?
- Possible solution : stereographic dilation on $\mathbb{S}^2$

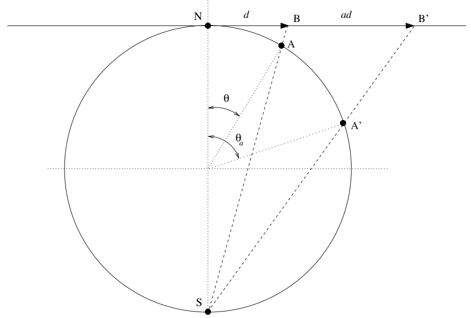

- Realization by unitary operators in $L^2(\mathbb{S}^2, d\mu)$:

$$. \text{ rotation } R_\varrho \ : \ (R_\varrho f)(\omega) \ = \ f(\varrho^{-1}\omega), \ \varrho \in \mathrm{SO}(3)$$

$$. \text{ dilation } D_a \ : \ (D_a f)(\omega) \ = \ \lambda(a,\theta)^{1/2} f(\omega_{1/a}), \quad a \in \mathbb{R}^*_+$$

where

  - $\omega_a \equiv (\theta_a, \varphi), \ a > 0$
  - θ_a is defined by $\tan \frac{\theta_a}{2} = a \tan \frac{\theta}{2}$
  - the normalization factor (cocycle, Radon-Nikodym derivative) is needed for compensating the noninvariance of the measure $d\mu$ under dilation :

$$\lambda(a,\theta) = \frac{4a^2}{[(a^2-1)\cos\theta + (a^2+1)]^2}$$

  - ϱ may be factorized into 3 rotations (Euler angles):

$$R_\varrho = R^z_\varphi \, R^y_\theta \, R^z_\gamma, \quad \varphi, \gamma \in [0, 2\pi), \ \theta \in [0, \pi]$$

General (coherent states) formalism: group of affine transformations on $\mathbb{S}^2$?

- Note :
  - motions $\varrho \in \mathrm{SO}(3)$ and dilations by $a \in \mathbb{R}^+_*$ do not commute
  - $\nexists$ semidirect product of SO(3) and $\mathbb{R}^+_*$ $\Rightarrow$ the only extension of SO(3) by $\mathbb{R}^+_*$ is their direct product
  - way out : embed the two factors into the Lorentz group $\mathrm{SO}_o(3,1)$, by the Iwasawa decomposition:

$$\mathrm{SO}_o(3,1) = \mathrm{SO}(3) \cdot A \cdot N,$$

where $A \sim \mathrm{SO}_o(1,1) \sim \mathbb{R} \sim \mathbb{R}^+_*$ (boosts in the z-direction) and $N \sim \mathbb{C}$

- Justification : the Lorentz group $\mathrm{SO}_o(3,1)$ is the conformal group both of the sphere $\mathbb{S}^2$ and of the tangent plane $\mathbb{R}^2$

- Action of Lorentz group :
  - Stability subgroup of the North Pole : $P = \mathrm{SO}_z(2) \cdot A \cdot N$ (minimal parabolic subgroup)
    $\Rightarrow \mathbb{S}^2 \simeq \mathrm{SO}_o(3,1)/P \simeq \mathrm{SO}(3)/\mathrm{SO}(2)$
    $\Rightarrow \mathrm{SO}_o(3,1)$ acts transitively on $\mathbb{S}^2$
  - explicit computation (with Iwasawa decomposition) :
    pure dilation = boost in z-direction = stereographic dilation !
- Natural UIR of Lorentz group $\mathrm{SO}_o(3,1)$ in Hilbert space $L^2(\mathbb{S}^2, d\mu)$:

$$[U(g)f](\omega) = \lambda(g,\omega)^{1/2} f\left(g^{-1}\omega\right), \ g \in \mathrm{SO}_o(3,1), \ f \in L^2(\mathbb{S}^2, d\mu),$$

where $\lambda(g,\omega)$ = Radon-Nikodym derivative

- Parameter space of spherical wavelets :

$$X = \mathrm{SO}_o(3,1)/N \simeq \mathrm{SO}(3) \cdot \mathbb{R}^+_*$$

$\Rightarrow$ introduce section $\sigma \ : \ X = \mathrm{SO}_o(3,1)/N \to \mathrm{SO}_o(3,1)$

and consider reduced representation $U(\sigma(\varrho, a))$

- Natural (Iwasawa) section : $\sigma(\varrho, a) = \varrho\, a, \ \varrho \in \mathrm{SO}(3), \ a \in A$.
  $\Rightarrow \ U(\sigma(\varrho, a)) = U(\varrho\, a) = U(\varrho)U(a) = R_\varrho\, D_a$ as before !

- The UIR is square integrable on X, that is, there exists nonzero (admissible) vectors $\psi \in L^2(\mathbb{S}^2, d\mu)$ such that

$$\int_X |\langle U(\sigma(\varrho, a))\psi|\phi\rangle|^2 \, \frac{da}{a^3} \, d\varrho := \langle \phi | A_\psi \phi \rangle < \infty, \ \forall \, \phi \in L^2(\mathbb{S}^2, d\mu) \,,$$

where $d\varrho$ = left Haar measure on SO(3)

- Resolution operator A_ψ is diagonal in Fourier space (Fourier multiplier):

$$\widehat{A_\psi f}(l,m) = G_\psi(l) \widehat{f}(l,m)$$

where

$$G_\psi(l) = \frac{8\pi^2}{2l+1} \sum_{|m| \leqslant l} \int_0^\infty |\widehat{\psi}_a(l,m)|^2 \, \frac{da}{a^3}, \quad \forall \, l \in \mathbb{N},$$

and $\widehat{\psi}_a(l,m) = \langle Y_l^m | \psi_a \rangle$ is the Fourier coefficient of $\psi_a = D_a \psi$

The group-theoretical method : Result # 2

- Admissible wavelet = function $\psi \in L^2(\mathbb{S}^2, d\mu)$ for which $\exists\, c > 0$ such that

$$G_\psi(l) \leqslant c, \quad \forall\, l \in \mathbb{N},$$

$\Leftrightarrow$ the resolution operator A_ψ is bounded and invertible

- Weak admissibility condition on ψ:

$$\int_{\mathbb{S}^2} \frac{\psi(\theta,\varphi)}{1+\cos\theta}\, d\mu(\theta,\varphi) = 0 \qquad + \text{ regularity conditions}$$

similar to the "zero mean" condition of ψ on the line/plane.

$\Rightarrow$ the spherical CWT acts as a local filter, as in the flat case !

The group-theoretical method : Result # 3

- For any admissible ψ such that $\int_0^{2\pi} \psi(\theta,\varphi)\, d\varphi \not\equiv 0$, the family $\{\psi_{a,\varrho} := R_\varrho D_a \psi,\ (\varrho, a) \in X\}$ is a continuous frame, that is, $\exists$ m > 0 and M $< \infty$ such that

$$\mathrm{m}\, \|\phi\|^2 \leqslant \int_X |\langle \psi_{a,\varrho} | \phi \rangle|^2 \frac{da}{a^3}\, d\varrho \leqslant \mathrm{M}\, \|\phi\|^2,\ \forall\, \phi \in L^2(\mathbb{S}^2, d\mu).$$

$\Leftrightarrow \quad \exists\, d > 0$ such that $d \leqslant G_\psi(l) \leqslant c, \quad \forall\, l \in \mathbb{N}$

$\Leftrightarrow \quad A_\psi$ and A_ψ^{-1} both bounded

- Note :
  - true for any axisymmetric (zonal) wavelet
  - frame probably not tight !

Example of admissible spherical wavelet

Difference of Gaussians spherical wavelet (SDOG)

$$\psi_G^{(\alpha)}(\theta,\varphi) = \phi(\theta,\varphi) - \tfrac{1}{\alpha}[D_\alpha \phi](\theta,\varphi), \quad \alpha > 0$$

where $\phi(\theta,\varphi) = \exp(-\tan^2(\frac{\theta}{2}))$

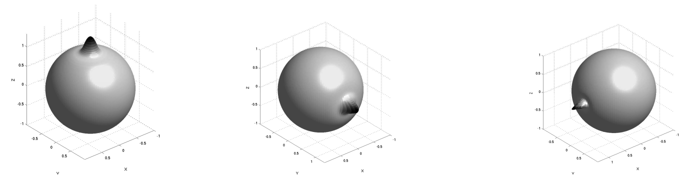

original ($a = 0.125$) rotated rotated and scaled ($a = 0.0625$)

The spherical DOG $\psi_G^{(\alpha)}$ wavelet, for $\alpha = 1.25$.

The Spherical CWT

- The Spherical CWT

$$W_f(\varrho, a) = \langle \psi_{a,\varrho} | f \rangle = \int_{\mathbb{S}^2} \overline{[R_\varrho D_a \psi](\omega)}\, f(\omega)\, d\mu(\omega)$$

ψ admissible wavelet, $f \in L^2(\mathbb{S}^2)$

- Reconstruction formula

For $f \in L^2(\mathbb{S}^2)$, ψ an admissible wavelet such that $\int_0^{2\pi} d\varphi\, \psi(\theta,\varphi) \neq 0$,

$$f(\omega) = \int_{\mathbb{R}_+^*} \int_{SO(3)} W_f(\varrho, a)\, [A_\psi^{-1} R_\varrho D_a \psi](\omega)\, \frac{da}{a^3}\, d\varrho$$

- Plancherel relation

$$\|f\|^2 = \int_{\mathbb{R}_+^*} \int_{SO(3)} \overline{\widetilde{W}_f(\varrho, a)}\, W_f(\varrho, a)\, \frac{da}{a^3}\, d\varrho$$

with

$$\widetilde{W}_f(\varrho, a) = \langle \widetilde{\psi}_{\varrho,a} | f \rangle = \langle A_\psi^{-1} R_\varrho D_a \psi | f \rangle$$

The Spherical CWT: the axisymmetric case

- General rotation : $\varrho = \varrho(\varphi, \theta, \alpha) \in \mathrm{SO}(3)$, Euler angles
- g axisymmetric $\Rightarrow R_\varrho g = R_{[\omega]} g$, where $[\omega] = \varrho(\varphi, \theta, 0)$

  $\therefore g$ localized around North Pole $\Rightarrow R_{[\omega]} g$ localized around $\omega = (\theta, \varphi)$

- Thus CWT redefined on $\mathbb{S}^2 \times \mathbb{R}_+^*$ by a spherical correlation

$$W_f(\omega, a) = (\psi_a \star f)(\omega) = \int_{\mathbb{S}^2} \overline{R_{[\omega]}\, \psi_a(\omega')}\, f(\omega')\, d\mu(\omega')$$

- New reconstruction formula

$$f(\omega) = \int_{\mathbb{R}_+^*} \int_{\mathbb{S}^2} W_f(\omega', a)\, [A_\psi^{-1} R_{[\omega]} D_a \psi](\omega')\, \frac{da}{a^3}\, d\mu(\omega')$$

An academic example

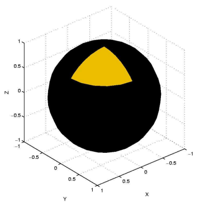

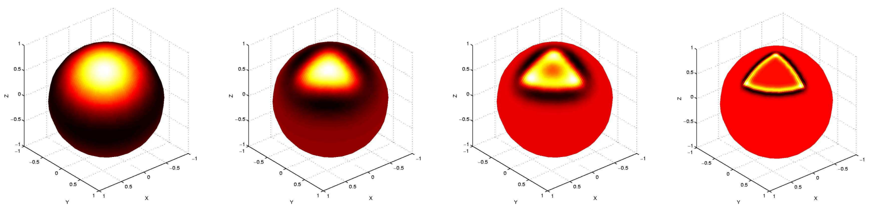

$a = 0.5$ $a = 0.2$ $a = 0.1$ $a = 0.035$

A real life example: analysis of the Milky Way

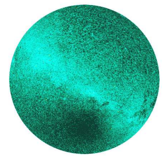

Original data: Hipparcos and Tycho Stars Catalogues

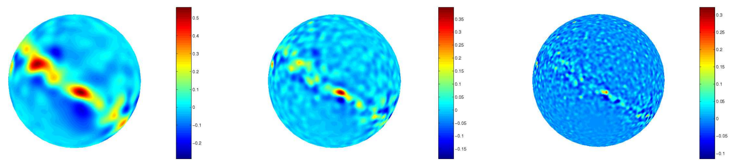

$W_f(\omega, 0.08)$ $W_f(\omega, 0.04)$ $W_f(\omega, 0.02)$

Another example: spherical map of Europe

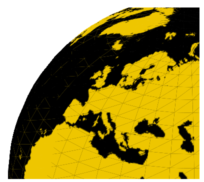

Original picture

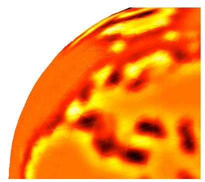

Wavelet transform at $a = 0.032$

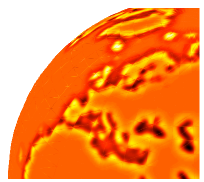

Wavelet transform at $a = 0.016$

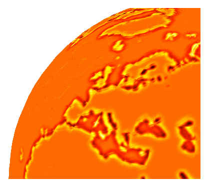

Wavelet transform at $a = 0.0082$

Note: WT at finest resolution has same artifacts as the original picture: closed strait of Gibraltar, unresolved complex Corsica–Sardinia, ragged coastlines, etc.

- Wanted: CWT on $\mathbb{S}^2$ tends locally to CWT on tangent plane
- Technique : group contraction along z-axis, with sphere radius as parameter ($R \to \infty$)
- For the groups

$$\begin{array}{rcl} SO(3) & \longrightarrow & \mathbb{R}^2 \rtimes SO(2) \\ SO_o(3,1) = SO(3) \cdot A \cdot N & \longrightarrow & \mathbb{R}^2 \rtimes SIM(2) \end{array}$$

- For the group actions

  Replace sphere $\mathbb{S}^2$ by sphere $\mathbb{S}^2_R$ of radius R, then:

  action of $\sigma(X) \subset SO_o(3,1)$ on $\mathbb{S}^2_R \longrightarrow$ action of SIM(2) on $\mathbb{R}^2$

- For the representations

  Define a family of representations U_R on $L^2(\mathbb{S}^2_R, d\omega_R)$ $(d\omega_R = R^2 d\omega)$

$$U_R(\gamma; a) = U(\sigma(\gamma; a/R))$$

  Then $U_R \longrightarrow U$ as $R \to \infty$ (strong limit on a dense set)

- For the CWT on $\mathbb{S}^2$

  Let $\psi(\vec{x}) \in L^2(\mathbb{R}^2, d^2\vec{x})$ and $\psi_R = \pi_R^{-1}\psi$, where

$$\pi_R : L^2(\mathbb{S}^2_R, d\omega_R) \to L^2(\mathbb{R}^2, d^2\vec{x})$$

  is the unitary map induced by the stereographic projection. Then

$$G_{\psi_R}(l) \leqslant c \; (\forall\, l \in \mathbb{N}) \quad \xrightarrow{R\to\infty} \quad c_\psi \sim \int |\widehat{\psi}(\vec{k})|^2 \, \frac{d^2\vec{k}}{|\vec{k}|^2} < \infty$$

  Thus admissible vectors on $\mathbb{S}^2$ correspond to admissible vectors on $\mathbb{R}^2$, i.e., the Euclidean limit holds : for $\psi = \lim_{R\to\infty} \pi_R \psi_R$,

$$\begin{array}{ccc} \psi_R \text{ admissible on } \mathbb{S}^2_R & \Longrightarrow & \displaystyle\int_{\mathbb{S}^2_R} \frac{\psi_R(\omega)}{1+\cos\theta}\, d\omega_R = 0 \\ \Downarrow & & \Downarrow \\ \psi \text{ admissible on } \mathbb{R}^2 & \Longrightarrow & \displaystyle\int \psi(\vec{x})\, d^2\vec{x} = 0 \end{array}$$

  Example:

  SDOG wavelet on $\mathbb{S}^2_R \Longrightarrow$ DOG wavelet on $\mathbb{R}^2$

The geometrical or conformal method

- Group-theoretical method yields only asymptotic connection with plane CWT (Euclidean limit : $R \to \infty$)
- There is a direct connection through inverse stereographic projection
- . . . and it is uniquely specified by geometrical considerations !

$\Rightarrow$ it is possible to obtain uniquely the same spherical CWT from the plane (Euclidean) one, simply by lifting everything from the tangent plane to the sphere by inverse stereographic projection:

- Wavelets
- Admissibility conditions
- Directionality or steerability properties

- Uniqueness of the stereographic projection
  - Let $\mathrm{p} : \mathbb{S}^2 \to \mathbb{R}^2$ be a radial diffeomorphism from the 2-sphere to the tangent plane at the North Pole:

$$\mathrm{p}(\theta, \varphi) = (r(\theta), \varphi) \quad \text{with inverse} \quad \mathrm{p}^{-1}(r, \varphi) = (\theta(r), \varphi)$$

  - Assume that p is a conformal map, i.e., it preserves angles, or the metric g' induced by p on $\mathbb{R}^2$ is conformally equivalent to the Euclidean metric g:

$$g'_{ij}(r, \varphi) = e^{\phi(r)}\, g_{ij}(r, \varphi), \quad \phi(r) > 0$$

  - Then $r(\theta) = 2\tan\frac{\theta}{2}$, i.e., p is the stereographic projection

- Uniqueness of the stereographic dilation
  - Let D_a be a radial dilation on the sphere $\mathbb{S}^2$:

$$D_a(\theta, \varphi) = (\theta_a(\theta), \varphi)$$

    Assume D_a is a conformal diffeomorphism
  - Then one has uniquely :

$$\tan(\frac{\theta_a}{2}) = a\tan(\frac{\theta}{2}), \quad \text{i.e., } D_a \text{ is the stereographic dilation}$$

Construction of the spherical CWT : The geometrical or conformal method

Thus one obtains an equivalence principle between the two wavelet formalisms :

- Let $\pi : L^2(\mathbb{S}^2, d\omega) \to L^2(\mathbb{R}^2, d^2\vec{x})$ be the unitary map induced by the stereographic projection :

$$[\pi F](\vec{x}) = \frac{1}{1+(r/2)^2} F(\mathrm{p}^{-1}(\vec{x})), \quad F \in L^2(\mathbb{S}^2, d\omega)$$

  with inverse

$$[\pi^{-1} f](\theta, \varphi) = \frac{2}{1+\cos\theta} f(\mathrm{p}(\theta,\varphi)), \quad f \in L^2(\mathbb{R}^2, d^2\vec{x})$$

- Then every admissible Euclidean wavelet $\psi \in L^2(\mathbb{R}^2, d^2\vec{x})$ yields an admissible spherical wavelet $\pi^{-1}\psi \in L^2(\mathbb{S}^2, d\omega)$
- In particular, if ψ is a directional wavelet, so is $\pi^{-1}\psi$

Example : The spherical Morlet wavelet (real part)

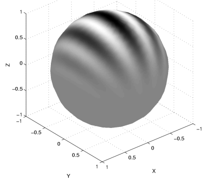

$a = 0.3$

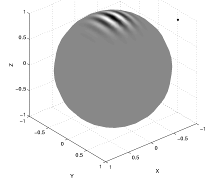

$a = 0.03$

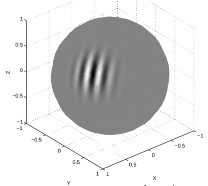

$a = 0.03$, center at $(\pi/3, \pi/3)$

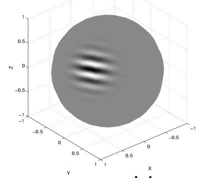

The same, rotated by $\pi/2$

Analysis of the same triangle with the spherical Morlet wavelet ($\alpha = 1.25$)

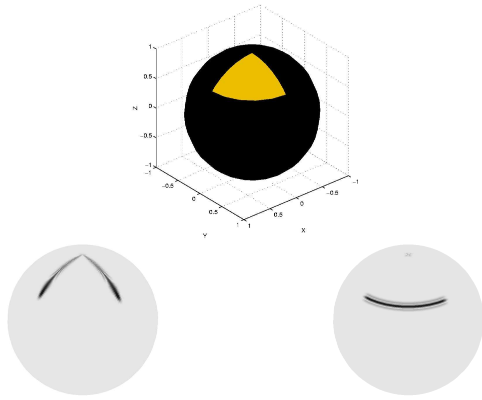

$\chi = 0^\circ$ $\chi = 90^\circ$

Wavelet frames on the 2-sphere

Different notions of frame (equivalent mathematically, not numerically!)

- Classical frame $\{\psi_n\} \in \mathfrak{H}$:

$$\mathrm{m}\,\|f\|^2 \leqslant \sum_{n\in\Gamma} |\langle\psi_n|f\rangle|^2 \leqslant \mathrm{M}\,\|f\|^2, \ \forall f \in \mathfrak{H}$$

- Controlled frame :

$$\mathrm{m}\,\|f\|^2 \leqslant \sum_{n\in\Gamma} \langle\psi_n|f\rangle \langle f|\,C\,\psi_n\rangle \leqslant \mathrm{M}\,\|f\|^2, \ \forall f \in \mathfrak{H}$$

  where $C \in GL(\mathfrak{H})$: bounded, bounded inverse
- Weighted frame :

$$\mathrm{m}\,\|f\|^2 \leqslant \sum_{n\in\Gamma} w_n\,|\langle\psi_n|f\rangle|^2 \leqslant \mathrm{M}\,\|f\|^2, \ \forall f \in \mathfrak{H}$$

  $w_n > 0$: weights (diagonalize C!)

Approach # 1 : weighted frame

- ψ = axisymmetric wavelet (throughout)
- Half-continuous grid $\Lambda = \{(\omega, a_j) : \omega \in \mathbb{S}^2, j \in \mathbb{Z}, a_j > a_{j+1}\}$
- Want :

$$\mathsf{m}\, \|f\|^2 \;\leqslant\; \sum_{j\in\mathbb{Z}} \nu_j \int_{\mathbb{S}^2} |W_f(\omega, a_j)|^2 \, d\mu(\omega) \;\leqslant\; \mathsf{M}\, \|f\|^2$$

$\Leftrightarrow \{\psi_{\omega,a_j} = R_{[\omega]} D_{a_j} \psi : (\omega, a_j) \in \Lambda\}$ = half-continuous frame in $L^2(\mathbb{S}^2)$

- Sufficient condition :

$$\mathsf{m} \;\leqslant\; \frac{4\pi}{2l+1} \sum_{j\in\mathbb{Z}} \nu_j \, |\widehat{\psi}_{a_j}(l,0)|^2 \;\leqslant\; \mathsf{M}$$

Example:

- SDOG wavelet ($\alpha = 1.25$),
- discretized dyadic scale with K voices $a_j = a_0\, 2^{-j/K}$, $\quad j \in \mathbb{Z}$
- weights adapted to natural measure $a^{-3} da$:

$$\nu_j = \frac{a_j - a_{j+1}}{a_j^3} = a_j^{-2} \left(\tfrac{2^{1/K} - 1}{2^{1/K}}\right)$$

- frame bounds m, M estimated from minimum and maximum of quantity

$$S(l) = \frac{4\pi}{2l+1} \sum_{j\in\mathbb{Z}} \nu_j |\widehat{\psi}_{a_j}(l,0)|^2 \text{ over } l \in [0,31] \text{ and for } K \in [1,4]$$

- Result :

K	m	M	M/m
1	0.5281	0.9658	1.8288
2	0.6817	1.1203	1.8107
3	0.6537	1.1836	1.8107
4	0.6722	1.2171	1.8107

$\therefore$ ratio M/m $\to$ 1.8107 : nontight frame !

- Reason : resolution operator A_ψ not taken into account

Approach # 2 : controlled frame

- Want :

$$\mathsf{m}\, \|f\|^2 \;\leqslant\; \sum_{j\in\mathbb{Z}} \nu_j \int_{\mathbb{S}^2} W_f(\omega, a_j)\, \overline{\widetilde{W_f}(\omega, a_j)} \, d\mu(\omega) \;\leqslant\; \mathsf{M}\, \|f\|^2$$

$$\widetilde{W_f}(\varrho, a) = \langle A_\psi^{-1} R_\varrho D_a \psi | f \rangle$$

- Sufficient condition :

$$\mathsf{m} \;\leqslant\; \frac{4\pi}{2l+1} G_\psi(l)^{-1} \sum_{j\in\mathbb{Z}} \nu_j \, |\widehat{\psi}_{a_j}(l,0)|^2 \leqslant \mathsf{M}$$

Example : Same SDOG wavelet as in approach # 1
Result :

K	m	M	M/m
1	0.7313	0.7628	1.0431
2	0.8747	0.8766	1.0021
3	0.9242	0.9254	1.0014
4	0.9503	0.9512	1.0009

$\therefore$ ratio M/m $\to 1$: a tight frame might be obtained

Construction of a tight half-continuous frame

Assume ψ is an axisymmetric wavelet such that

$$g_\psi(l) = \frac{4\pi}{2l+1} \sum_{j\in\mathbb{Z}} \nu_j \, |\widehat{\psi}_{a_j}(l,0)|^2 \neq 0, \ \forall\, l \in \mathbb{N}$$

Then

$$f(\omega) \;=\; \sum_{j\in\mathbb{Z}} \nu_j \, [W_f(\cdot, a_j) \star \psi^{\#}_{a_j}](\omega)$$

where

- $\psi^{\#}_{a_j} = A_\psi^{-1} D_{a_j} \psi$
- A_ψ = resolution operator defined by $\widehat{l_\psi^{-1} h}(l,m) = g_\psi^{-1}(l) h(l,m)$

  (discretization of continuous resolution operator A_ψ)

$\Rightarrow$ tight frame controlled by A_ψ^{-1}

- Discretization of scales : as before

$$a \in A = \{a_j \in \mathbb{R}_+^* : a_j > a_{j+1}, j \in \mathbb{Z}\}$$

- Discretization of positions : equi-angular grid $\mathcal{G}_j$, $j \in \mathbb{Z}$

$$\mathcal{G}_j = \{\omega_{jpq} = (\theta_{jp}, \varphi_{jq}) \in \mathbb{S}^2 : \theta_{jp} = \tfrac{(2p+1)\pi}{4B_j}, \varphi_{jq} = \tfrac{q\pi}{B_j}\}$$

$p, q \in \mathcal{N}_j := \{n \in \mathbb{N} : n < 2B_j\}$, $B_j \in \mathbb{N}, j \in \mathbb{Z}, B_j \in B$

- $\{\theta_{jp}\}$ = pseudo-spectral grid, with nodes on the zeros of a Chebyshev polynomial of order $2B_j$

$\Rightarrow$ (exact) quadrature rule (Driscoll-Healy)

$$\int_{\mathbb{S}^2} f(\omega)\, d\mu(\omega) = \sum_{p,q \in \mathcal{N}_j} w_{jp}\, f(\omega_{jpq}),$$

for certain weights $w_{jp} > 0$ and for every band-limited function $f \in L^2(\mathbb{S}^2)$ of bandwidth B_j (i.e., $\widehat{f}(l,m) = 0$ for all $l \geqslant B_j$)

$\Rightarrow$ complete space of discretization :

$$\Lambda(A, B) = \{(a_j, \omega_{jpq}) : j \in \mathbb{Z},\ p, q \in \mathcal{N}_j\}$$

- Want : weighted frame controlled by A_ψ^{-1}

$$\mathrm{m}\, \|f\|^2 \leqslant \sum_{j \in \mathbb{Z}} \sum_{p,q \in \mathcal{N}_j} \nu_j w_{jp}\, W_f(\omega_{jpq}, a_j)\, \overline{\widetilde{W}_f(\omega_{jpq}, a_j)} \leqslant \mathrm{M}\, \|f\|^2 \qquad (**)$$

- Sufficient condition : Let

$$S'(l) = \sum_{j \in \mathbb{Z}} \tfrac{4\pi\nu_j}{2l+1}\, \mathbb{1}_{[0,B_j)}(l)\ G_\psi^{-1}(l)\ |\widehat{\psi}_{a_j}(l,0)|^2,$$

$$\delta = \|\mathcal{X}\| \equiv \sup_{(H_l)_{l \in \mathbb{N}}} \frac{\|\mathcal{X} H\|}{\|H\|},$$

with the infinite matrix $(\mathcal{X}_{ll'})_{l,l' \in \mathbb{N}}$ given by

$$\mathcal{X}_{ll'} = \sum_{j \in \mathbb{N}} c_j(l,l')\, \mathbb{1}_{[2B_j,+\infty)}(l+l')\, |\widehat{\psi}_{a_j}(l,0)|\, |\widehat{\psi}_{a_j}(l',0)|$$

and $c_j(l,l') = \frac{2\pi\nu_j}{B_j}\, G_\psi^{-1}(l) \big[(2(l+B_j)+1)(2(l'+B_j)+1)\big]^{\frac{1}{2}}$.

Let $K_0 = \inf_{l \in \mathbb{N}} S'(l)$ and $K_1 = \sup_{l \in \mathbb{N}} S'(l)$. If one has

$$0 \leqslant \delta < K_0 \leqslant K_1 < \infty,$$

then the family $\{\psi_{jpq} = R_{[\omega_{jpq}]} D_{a_j} \psi : j \in \mathbb{Z},\ p, q \in \mathcal{N}_j\}$ is a weighted spherical frame controlled by the operator A_ψ^{-1} (i.e., (**) holds), with frames bounds $K_0 - \delta$, $K_0 + \delta$.

Note :

- $\|\mathcal{X}\|$ difficult to compute (infinite dimensional matrix)
- $f \in L^2(\mathbb{S}^2)$ band-limited of bandwidth $b \in \mathbb{N}^0$

$\Rightarrow$ $\mathcal{X}$ is $b \times b$-dimensional

Result :

- spherical DOG wavelet frame
- $b = 64$, dyadically discretized scale with $K = a_0 = 1$
- bandwidth associated to grid size at resolution j : $B_j = B_0 2^{|j|}$, $B_0 \in \mathbb{N}$, where B_0 is the minimal bandwidth associated to ψ_1.

Then one gets

	K_0	K_1	δ	$\mathrm{m} = K_0 - \delta$	$\mathrm{M} = K_1 + \delta$	M/m
$B_0 = 2$	0.6807	0.7700	84.1502	–	–	–
$B_0 = 4$	0.7402	0.7790	0.0594	0.6808	0.8384	1.2314
$B_0 = 8$	0.7402	0.7790	0.0014	0.7388	0.7804	1.0564

Conclusion :

- sufficient condition $0 \leqslant \delta < K_0 \leqslant K_1 < \infty$ satisfied for $B_0 \geqslant 4$
- but a tight frame cannot be obtained by increasing B_0
- for $B_0 \to \infty$, spherical grids get finer and finer $\Rightarrow$ half-continuous frame with one voice discretization of scale : not sufficient to get a tight frame !

Example #1 : Local enhancement of Jupiter's Red Spot

- Tools :
  - . SpharmonicKit (Rockmore et al.)
  - . MATLAB© YAWtb toolbox (UCL)
- Half-continuous spherical frame with SDOG wavelet, data bandwith $b = 256$, equi-angular grid of size 512×512

  $\Rightarrow$ good discretization for $|j| \leqslant 7$ and $a_0 = 1$
- Technique :
  - Before reconstruction, coefficients at the finest scale $W_f(\omega, a_7)$ are multiplied by a Gaussian mask $M(\omega) = 1 + n_{a'}[R_{[\omega']} D_{a'} G](\omega)$ localized on the center ω' of the Spot, with $\|M\|_{\infty=2}$
  - Mask increases their amplitudes by $\leqslant 2$ in vicinity of Red Spot
  - The rest of the coefficients are not modified

  Impossible to do with a purely frequential spherical decomposition !

Example #1 : Local enhancement of Jupiter's Red Spot

Result :

Original image

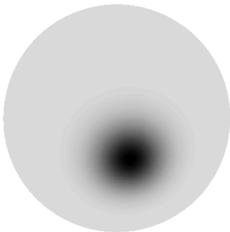

Local mask

Zoom over the Red Spot

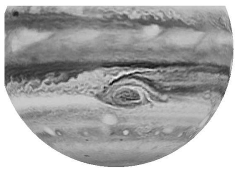

Zoom over the Red Spot with sharper details

Example #2 : Map of the Earth

- Original data f : World map, recorded on a equi-angular grid of 512×512 points
- Reconstruction ($|j| \leqslant 6$) with half-continuous spherical frame and SDOG wavelet, as before : relative error = 1.1%
- Combination of reconstruction with conjugate gradient algorithm (3 iterations) : relative error = 10^{-5} %

Example #2 : Map of the Earth

Result : SDOG coefficients $W_j[p, q] = W_j(\omega_{jpq})$

World map
(green $\simeq 1$, blue $\simeq 0$)

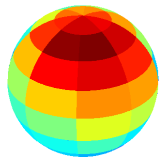

$W_0[p, q]$

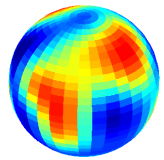

$W_2[p, q]$

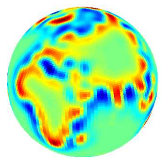

$W_4[p, q]$

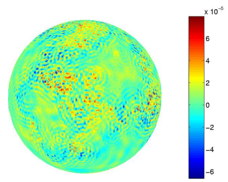

Difference between original data and reconstruction (scale 10^{-5})

The spherical CWT via stereographic projection

- Advantages:
  - easy to implement, if wavelet ψ is given explicitly
  - large freedom in choosing the mother wavelet ψ
  - allows use of directional wavelets
  - smoothness
- Disadvantages:
  - frames, not bases $\Longrightarrow$ redundancy $\Longrightarrow$ higher computing cost, not suitable for large amount of data
  - frames are applicable to band-limited functions only
  - problem of finding an appropriate discretization grid which leads to good frames
  - an explicit mother wavelet ψ cannot be continuous, locally supported and orthogonal at the same time

Orthogonal wavelet bases on the 2-sphere

Idea : exploit unitary map $\pi^{-1} : L^2(\mathbb{R}^2, d^2\vec{x}) \to L^2(\mathbb{S}^2, d\omega)$ to lift orthogonal wavelet bases from the tangent plane to the sphere

- Pointed sphere :

$$\dot{\mathbb{S}}^2 = \{(\eta_1, \eta_2, \eta_3) \in \mathbb{R}^3, \quad \eta_1^2 + \eta_2^2 + (\eta_3^2 - 1)^2 = 1\} \setminus \{(0,0,2)\}$$

  Parametrization:

$$\begin{aligned} \eta_1 &= \cos\varphi \sin\theta \\ \eta_2 &= \sin\varphi \sin\theta, \qquad \theta \in (0,\pi], \varphi \in [0, 2\pi) \\ \eta_3 &= 1 + \cos\theta \end{aligned}$$

- $\mathrm{p} : \dot{\mathbb{S}}^2 \to \mathbb{R}^2$: stereographic projection from North Pole $N(0,0,2)$ onto tangent plane at South Pole
- Area elements of $\mathbb{R}^2$ and $\mathbb{S}^2$: $d\vec{x} = \nu(\boldsymbol{\eta})^2 \, d\mu(\boldsymbol{\eta})$, with $\nu : \dot{\mathbb{S}}^2 \to \mathbb{R}$ defined as

$$\nu(\boldsymbol{\eta}) = \frac{2}{2 - \eta_3} = \frac{2}{1 - \cos\theta}, \quad \boldsymbol{\eta} = (\eta_1, \eta_2, \eta_3) \equiv (\theta, \varphi) \in \dot{\mathbb{S}}^2$$

Note : $L^2(\dot{\mathbb{S}}^2) := L^2(\dot{\mathbb{S}}^2, d\mu(\boldsymbol{\eta})) = L^2(\mathbb{S}^2)$, since $\mu(\{N\}) = 0$

Orthogonal wavelet bases on the 2-sphere

- The stereographic projection induces a map $\pi : L^2(\dot{\mathbb{S}}^2) \to L^2(\mathbb{R}^2)$ with inverse $\pi^{-1} : L^2(\mathbb{R}^2) \to L^2(\dot{\mathbb{S}}^2)$:

$$[\pi^{-1} F](\boldsymbol{\eta}) = \nu(\boldsymbol{\eta}) F(\mathrm{p}(\boldsymbol{\eta})), \text{ for all } F \in L^2(\mathbb{R}^2)$$

- π is a unitary map :

  to each $F \in L^2(\mathbb{R}^2)$, associate the function $F^s = \nu \cdot (F \circ \mathrm{p}) \in L^2(\dot{\mathbb{S}}^2)$
  Then

$$\langle F|G\rangle_{L^2(\mathbb{R}^2)} = \langle F^s|G^s\rangle_{L^2(\dot{\mathbb{S}}^2)}, \ \forall F, G \in L^2(\mathbb{R}^2).$$

- Consequences:
  - MRA/wavelet bases of $L^2(\mathbb{R}^2)$ $\rightsquigarrow$ MRA/wavelet bases of $L^2(\dot{\mathbb{S}}^2)$
  - orthogonal bases of $L^2(\mathbb{R}^2)$ $\rightsquigarrow$ orthogonal bases of $L^2(\dot{\mathbb{S}}^2)$
  - More precisely:

    F, G orthogonal in $L^2(\mathbb{R}^2)$ $\Longrightarrow$ F^s, G^s orthogonal in $L^2(\dot{\mathbb{S}}^2)$

Lifting everything to the sphere $\mathbb{S}^2$

- Choose a multiresolution analysis of $L^2(\mathbb{R}^2)$

$$\ldots \subset \mathbf{V}_{-2} \subset \mathbf{V}_{-1} \subset \mathbf{V}_0 \subset \mathbf{V}_1 \subset \mathbf{V}_2 \subset \ldots$$

  Then define $F \in L^2(\mathbb{R}^2) \longmapsto F^s = \nu \cdot (F \circ \mathrm{p}) \in \mathrm{L}^2(\mathbb{S}^2)$
- In particular,

$$F^s_{j,\mathbf{k}} = \nu \cdot (F_{j,\mathbf{k}} \circ \mathrm{p}), \text{ for } j \in \mathbb{Z}, \ \mathbf{k} \in \mathbb{Z}^2$$

- Taking $F = \Phi$ and $F = \Psi$,

$$\begin{aligned} \Phi^s_{j,\mathbf{k}} &= \nu \cdot (\Phi_{j,\mathbf{k}} \circ \mathrm{p}) \\ \Psi^s_{j,\mathbf{k}} &= \nu \cdot (\Psi_{j,\mathbf{k}} \circ \mathrm{p}) \end{aligned}$$

- For $j \in \mathbb{Z}$, we define $\mathcal{V}_j$ as

$$\mathcal{V}_j = \{\nu \cdot (F \circ \mathrm{p}), \ F \in \mathbf{V}_j\}.$$

Then

(1) $\mathcal{V}^j \subset \mathcal{V}^{j+1}$ for $j \in \mathbb{Z}$ and $\mathcal{V}^j$ closed subspaces of $L^2(\dot{\mathbb{S}}^2)$

(2) $\bigcap_{j\in\mathbb{Z}} \mathcal{V}^j = \{0\}, \quad \overline{\bigcup_{j\in\mathbb{Z}} \mathcal{V}^j} = L^2(\dot{\mathbb{S}}^2)$

(3) $\{\Phi_{0,\mathbf{k}},\ \mathbf{k} \in \mathbb{Z}^2\} = \text{ONB of } V^0 \Longrightarrow \{\Phi^s_{0,\mathbf{k}},\ \mathbf{k} \in \mathbb{Z}^2\} = \text{ONB of } \mathcal{V}^0$

A sequence $(\mathcal{V}^j)_{j\in\mathbb{Z}}$ of subspaces of $L^2(\dot{\mathbb{S}}^2)$ satisfying (1), (2), (3) constitutes a multiresolution analysis of $L^2(\dot{\mathbb{S}}^2)$

- Define the wavelet spaces $\mathcal{W}^j = \mathcal{V}^{j+1} \ominus \mathcal{V}^j$
- If $\{\Psi_{j,l},\ l \in J\}$ is a basis (resp. ONB) of $\mathbf{W}^j$, then

$$\{\Psi^s_{j,l},\ l \in J\} = \text{basis (resp. ONB) of } \mathcal{W}^j$$

$$\{\Psi^s_{j,l},\ l \in J,\ j \in \mathbb{Z}\} = \text{basis (resp. ONB) of } \overline{\oplus_{j\in\mathbb{Z}} \mathcal{W}^j} = L^2(\mathbb{S}^2)$$

$$(\text{here } J = \{(\mathbf{k}, \lambda) : \mathbf{k} \in \mathbb{Z}^2, \lambda = h, v, d\})$$

Conclusion:

- Φ has compact support in $\mathbb{R}^2 \Rightarrow \Phi^s_{j,\mathbf{k}}$ has local support on $\mathbb{S}^2$

  $$(\text{ diam supp } \Phi^s_{j,\mathbf{k}} \overset{j\to\infty}{\longrightarrow} 0 \ )$$

- orthonormal 2-D wavelet basis

  $\Rightarrow$ orthonormal spherical wavelet basis
- smooth 2-D wavelets $\Rightarrow$ smooth spherical wavelets
- In particular:
  Daubechies wavelets $\Rightarrow$ locally supported & orthonormal wavelets on $\mathbb{S}^2$
- decomposition & reconstruction matrices: the same tools as in plane 2-D case can be used ($\exists$ toolboxes)

- Take the following axisymmetric (or zonal) function on $\mathbb{S}^2$:

$$f(\theta, \varphi) = \begin{cases} 1, & \theta \leqslant \frac{\pi}{2} \\ (1 + 3\cos^2\theta)^{-1/2}, & \theta \geqslant \frac{\pi}{2} \end{cases}$$

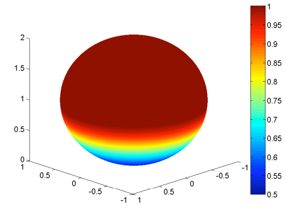

- This function and its gradient are continuous, but the second partial derivative with respect to θ has a discontinuity on the equator $\theta = \frac{\pi}{2}$

- Detecting properly such a discontinuity requires a wavelet with two vanishing moments at least :

  none of the methods described above would do in practice !
- Discretized CWT :
  - The spherical DOG wavelet does not detect the discontinuity : not enough vanishing moments
  - Analysis with the spherical wavelet $\Psi^s_{H_2}$ associated to the planar wavelet, with vanishing moments up to order 3 :

$$\Psi_{H2}(\vec{x}) = \Delta^2 e^{-\frac{1}{2}|\vec{x}|^2},$$
$$= (|\vec{x}|^4 - 8|\vec{x}|^2 + 8)e^{-\frac{1}{2}|\vec{x}|^2}$$

- Then analysis with db3 lifted onto $\dot{\mathbb{S}}^2$ as above

Example : Function with discontinuous second derivative

Analysis of the function $f(\theta, \varphi)$ by the discretized CWT method with the wavelet $\Psi^s_{H_2}$

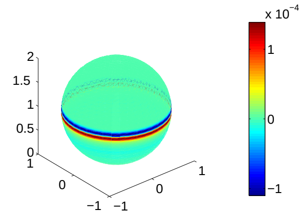

$a = 0.04$

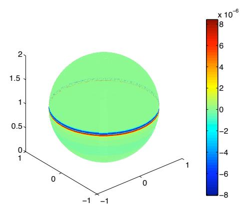

$a = 0.0165$

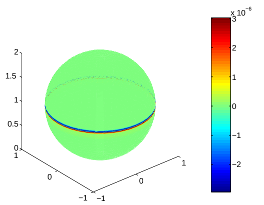

$a = 0.012$

Example : Function with discontinuous second derivative

- So, the detection performance improves when going down the scales ('zooming in') . . .
- . . . but there is a limit : when a becomes too small, the method fails (the wavelet becomes too small and 'falls in between' the discretization points)
- The same at scale 0.0085 :

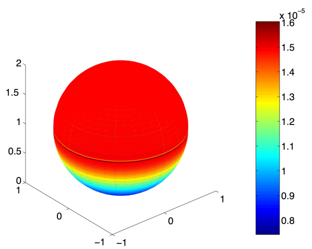

Example : Function with discontinuous second derivative

- On the contrary, a Daubechies wavelet db3 lifted on the sphere does the job better than the wavelet Ψ_{H2} :

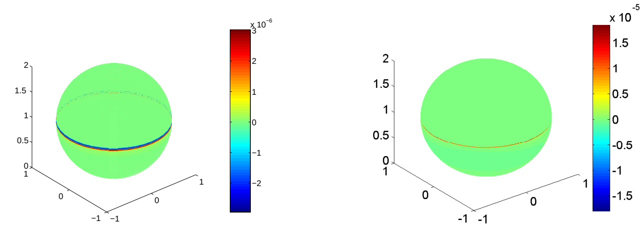

- The detection is much more precise, with less artefacts on the sides of the discontinuity : this is a consequence of the local support of the db3 wavelet, as opposed to the Gaussian tail of Ψ_{H2}
- Conclusion : a locally supported orthonormal wavelet basis may be lifted onto the sphere and it is more efficient for detecting a singularity than the discretized spherical CWT

DWT via stereographic projection

- Further advantage:
  - One can use all 2-D constructions, like ridgelets, curvelets, and so on
- Disadvantages:
  - One must avoid a region around a point (the North Pole N)
  - Deformations of the grid around N
- Possible generalization
  - The method works for any manifold with an orthogonal projection onto a fixed plane, that induces a unitary map between the respective L^2 spaces :
    - Upper sheet of two-sheeted hyperboloid with vertical projection onto plane $z = 0$
    - Same for paraboloid
  - Possible generalization to local analysis, e.g. on one hemisphere

THE CWT ON OTHER MANIFOLDS

The CWT on curved manifolds

- The two-sheeted hyperboloid : manifold dual to the sphere, constant negative curvature
  - Motions are OK : isometry group = $SO_o(2,1)$
  - Dilations are problematic : large stereographic dilations map upper sheet onto lower sheet ; several other methods available (projection onto tangent cone, onto equatorial plane, . . .)
  - But CWT can be derived using appropriate integral transform (Fourier-Helgason) that leads to convolution theorems
- The paraboloid : singular case! No large isometry group, possible time-frequency-like transform, not really a wavelet transform
- General conic sections : unified CWT for all 3 conic sections, using differential-geometric methods, promising approach, not yet complete

The CWT on other conic sections

- Apollonius : the (normalized) conic sections are
  - the sphere $\mathbb{S}^2$
  - the paraboloid $\mathbb{P}^2$
  - the two-sheeted hyperboloid $\mathbb{H}^2$
- All three are obtained as sections by a hyperplane of a double null-cone

$$\mathcal{C}_0^3 := \{(x_0, x_1, x_2, x_3) \in \mathbb{R}^4 : \; x_0^2 - x_1^2 - x_2^2 - x_3^2 = 0\}$$

- All conic sections may be obtained by varying the tilt angle α of the hyperplane intersecting the null-cone $\mathcal{C}_0^3$, i.e., writing the equation of the plane as $x_0 = 1 + \tan\alpha(x_3 - 2), \; \alpha \in [0, \pi/2]$

  In this way we get
  - $\mathbb{S}^2$ for $\alpha = 0$
  - ellipsoids for $\alpha \in (0, \pi/4)$
  - a paraboloid for $\alpha = \pi/4$
  - hyperboloids for $\alpha \in (\pi/4, \pi/2]$.

The CWT on the two-sheeted hyperboloid

[I. Bogdanova (PhD thesis, 2005), P. Vandergheynst (EPFL)]

- The two-sheeted hyperboloid $\mathbb{H}^2$ is the dual manifold of the sphere $\mathbb{S}^2$, with constant negative curvature and equation

$$x_0^2 - x_1^2 - x_2^2 = 1$$

- Parameterization of the upper sheet $\mathbb{H}^2_+ (x_0 \geqslant 1)$ is given by $\mathbf{x} = (x_0, x_1, x_2) = \mathbf{x}(\chi, \varphi)$, where

$$\begin{aligned} x_0 &= \cosh\chi \\ x_1 &= \sinh\chi\cos\varphi, \\ x_2 &= \sinh\chi\sin\varphi \end{aligned}$$

$(\chi \geqslant 0, \; 0 \leqslant \varphi < 2\pi)$

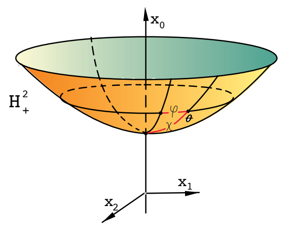

The CWT on the two-sheeted hyperboloid $\mathbb{H}^2$

Affine transformations on $\mathbb{H}^2_+$

- Motions on $\mathbb{H}^2_+$
  - (i) rotations : $\mathbf{x}(\chi,\varphi) \mapsto \mathbf{x}(\chi,\varphi+\varphi_0)$
  - (ii) hyperbolic motions : $\mathbf{x}(\chi,\varphi) \mapsto \mathbf{x}(\chi+\chi_0,\varphi)$

  Together they constitute the isometry group $\mathrm{SO}_o(2,1)$
- Dilations ??

  Requirement : Dilation = homeomorphism $\mathrm{d}_a : \mathbb{H}^2_+ \to \mathbb{H}^2_+$ such that
  - d_a monotonically dilates the azimuthal distance between two points
  - $\{\mathrm{d}_a, a>0\}$ is homomorphic to $\mathbb{R}^+_*$: $\mathrm{d}_a \mathrm{d}_b = \mathrm{d}_{ab}, \mathrm{d}_{a^{-1}} = \mathrm{d}_a^{-1}, \mathrm{d}_1 = I$

  Many possibilities !

Choice of hyperbolic dilation

(1) Dilation through stereographic projection

As for $\mathbb{S}^2$, one has a "pseudo-Iwasawa" decomposition:

$$\mathrm{SO}_o(3,1) = \mathrm{SO}_o(2,1)\cdot \mathbb{R}\cdot \mathrm{N},$$

where $\mathbb{R} \sim \mathrm{SO}_o(1,1) \sim$ boosts in the z-direction and $\mathrm{N} \sim \mathbb{C}$ By the same technique, one gets

$$\tanh\frac{\chi_a}{2} = a\tanh\frac{\chi}{2}$$

Problems :

- Since $|\tanh\chi| \leqslant 1$, there is a critical value χ_o such that all points (χ_o,φ) will be sent to infinity by a finite dilation $a_o = (\tanh\chi_o/2)^{-1}$
- Moreover, for $a > a_o$, the dilation maps the upper sheet $\mathbb{H}^2_+$ of the hyperboloid onto the lower sheet $\mathbb{H}^2_-$!

  Unacceptable for setting up a CWT !
- Also, there is no obvious representation of $\mathrm{SO}_o(3,1)$ in $L^2(\mathbb{H}^2_+)$

Choice of hyperbolic dilation

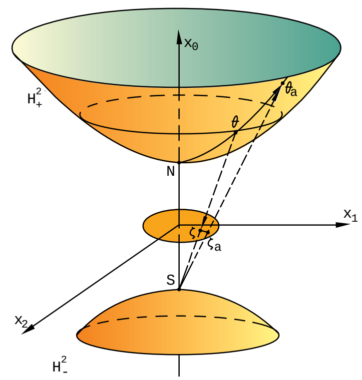

Under stereographic projection :

- Upper sheet $\mathbb{H}^2_+$ $\Leftrightarrow$ interior of unit disk
- Lower sheet $\mathbb{H}^2_-$ $\Leftrightarrow$ exterior of unit disk

Choice of hyperbolic dilation

(2) Dilation through conic projection

Idea : project the upper sheet of the hyperboloid $\mathbb{H}^2_+$ onto its tangent half null-cone $\mathcal{C}^2_+$

$$\mathcal{C}^2_+ := \{(x_0,x_1,x_2)\in\mathbb{R}^3 :\ x_0^2 - x_1^2 - x_2^2 = 0,\ x_0 \geqslant 0\},$$

with radial dilation $\mathbf{x} \mapsto a\,\mathbf{x}$

Conic projection : $\Phi : \mathbb{H}^2_+ \to \mathcal{C}^2_+$, given by

$$\Phi(x) = 2\sinh\frac{\chi}{2}\,e^{i\varphi}, \quad x = x(\chi,\varphi)$$

$\Longrightarrow$ dilation given by $\quad \sinh\dfrac{\chi_a}{2} = a\sinh\dfrac{\chi}{2}$

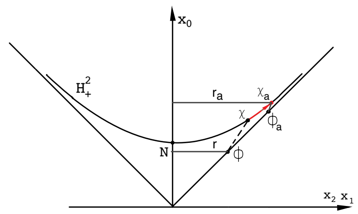

(3) Dilation through conic projection and "flattening"

Idea : project the cone $\mathcal{C}^2_+$ onto the plane $x_0 = 0$

- Conic projection + "flattening" : $\pi_0\Phi : \mathbb{H}^2_+ \to \mathbb{C}$, given by

$$\pi_0\Phi(x) = \sinh\chi\, e^{i\varphi}, \quad x = x(\chi,\varphi)$$

$\Longrightarrow$ dilation given by $\sinh\chi_a = a\sinh\chi$

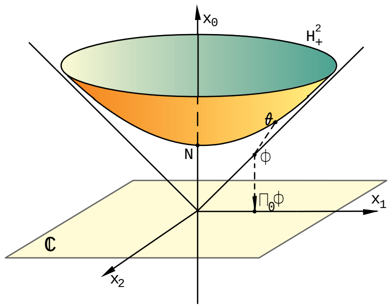

- Generalization : one-parameter family of possible projections

$$\pi_0\Phi(x) = \frac{1}{p}\sinh p\chi\, e^{i\varphi}, \quad x = x(\chi,\varphi)$$

$\Longrightarrow$ dilation given by $\sinh p\chi_a = a\sinh p\chi$

- $p = \frac{1}{2}$: dilation by conic projection
- $p = 1$: dilation by conic projection and flattening

- CWT on the hyperboloid

Idea : Exploit the existence of an appropriate integral transform on $L^2(\mathbb{H}^2_+)$, the Fourier-Helgason transform, that defines harmonic analysis on $\mathbb{H}^2$, including convolution theorems

- The FH-transform :

$$\widehat{f}(\nu,\xi) = \int_{\mathbb{H}^2_+} f(x)\,(x\cdot\xi)^{-\frac{1}{2}+i\nu}\,d\mu(x), \quad \forall f \in C^\infty_0(\mathbb{H}^2_+)$$

where

- $\mu = \mathrm{SO}_o(2,1)$-invariant measure on $\mathbb{H}^2_+$
- $\nu > 0, \xi \in \mathbb{P}\mathcal{C}_+ = \{\xi \in \mathcal{C}^2_+ : \lambda\xi \equiv \xi, \lambda > 0, \xi_0 > 0\}$ (projective forward cone)
- $(x\cdot\xi)^{-\frac{1}{2}-i\nu}$ = hyperbolic plane wave = eigenfunction of Laplacian over $\mathbb{H}^2_+$

- FH-transform extends to isometry of $L^2(\mathbb{H}^2_+, d\mu)$ onto $L^2(\mathcal{L}, d\eta)$
- Hyperbolic convolution : for $f \in L^2(\mathbb{H}^2_+)$ and $s \in L^1(H^2_+)$

$$(f * s)(y) = \int_{\mathbb{H}^2_+} f([y]^{-1}x)\,s(x)\,d\mu(x), \quad y \in \mathbb{H}^2_+$$

where one uses a section $[\cdot] : \mathbb{H}^2_+ \to \mathrm{SO}_o(2,1)$

- Convolution theorem :
let $f, s \in L^2(\mathbb{H}^2_+)$ with s rotation invariant. Then $s * f \in L^1(\mathbb{H}^2_+)$ and

$$\widehat{(s * f)}(\nu,\xi) = \widehat{f}(\nu,\xi)\widehat{s}(\nu)$$

- Hyperbolic CWT : looks exactly the same as its spherical counterpart:

$$W_f(a,g) = \langle\psi_{a,g}|f\rangle = \int_{\mathbb{H}^2_+} \overline{\psi_a(g^{-1}x)}\,f(x)\,d\mu(x),$$

where

- $\mu = \mathrm{SO}_o(2,1)$-invariant measure on $\mathbb{H}^2_+$
- $g \in \mathrm{SO}_o(2,1)$, $a > 0$
- $\psi_a(x) = \lambda(a,x)\psi(d_{1/a}x)$, with d_a an appropriate dilation and $\lambda(a,x)$ = normalization factor (Radon-Nikodym derivative) for compensating the noninvariance of the measure $d\mu$ under dilation

- If the wavelet ψ is axisymmetric, the HCWT is a convolution :

$$W_f(a,g) = W_f(a,[x]) = (\overline{\psi_a} * f)(x)$$

$\Longrightarrow$ reconstruction formula, as in the spherical case

The hyperbolic CWT

- Admissibility condition
  - $\psi \in L^1(\mathbb{H}^2_+)$, axisymmetric
  - α positive function on $\mathbb{R}^+_*$
  - $\exists$ constants m, M such that

$$0 < \mathrm{m} \leqslant \mathfrak{A}_\psi(\nu) = \int_0^\infty |\widehat{\psi_a}(\nu)|^2 \, \alpha(a) da \leqslant \mathrm{M} < \infty$$

- Then the resolution operator A_ψ defined by

$$A_\psi f(x') = \int_{\mathbb{H}^2_+} \int_0^\infty W_f(a,x) \psi_{a,[x]}(x') dx \, \alpha(a) da$$

is bounded with bounded inverse

- The resolution operator A_ψ is diagonal in Fourier–Helgason space (Fourier–Helgason multiplier):

$$\widehat{A_\psi f}(\nu, \xi) = \mathfrak{A}_\psi(\nu) \widehat{f}(\nu, \xi)$$

$\therefore$ The family $\{\psi_{a,[x]}, a > 0, x \in \mathbb{H}^2_+\}$ is a continuous frame

The hyperbolic CWT

- Reconstruction formula (in strong sense in $L^2(\mathbb{H}^2_+)$)

$$f(x') = \int_0^\infty \int_{\mathbb{H}^2_+} W_f(a,x) \, A_\psi^{-1} \psi_{a,[x]}(x') \, \alpha(a) da \, dx$$

- Choice of function α is arbitrary, up to admissibility

  Example :

  $\alpha(a) \sim a^{-\beta}, \beta > 0$, for large a $\Rightarrow$ ψ is p-admissible if $\beta > \dfrac{2}{p} + 1$

- Typical hyperbolic wavelet : hyperbolic DOG at scale a :

$$f_\psi(\chi, \varphi) = \frac{1}{a} \exp\Big[-\frac{1}{a^2} \sinh^2(\frac{\chi}{2}) \Big] - \frac{1}{4a} \exp\Big[-\frac{1}{4a^2} \sinh^2(\frac{\chi}{2}) \Big]$$

(dilation via conic projection)

The hyperbolic CWT

Action of hyperbolic translation on hyperbolic DOG at scale $a = 0.3$ and position $\varphi = \pi$

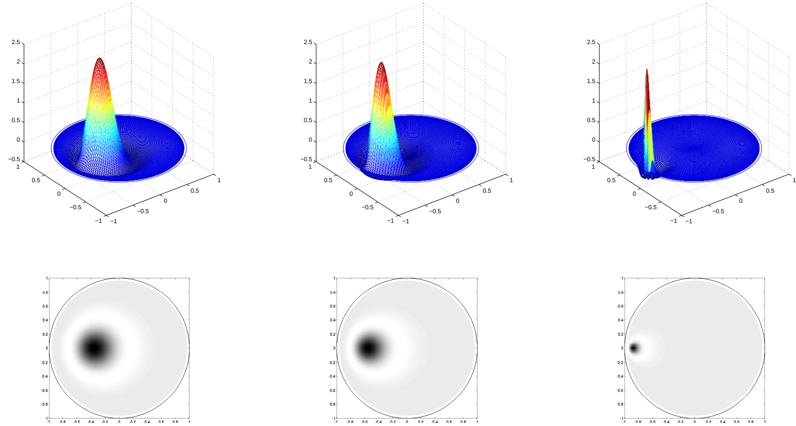

$\chi = 0.75$ $\chi = 1.25$ $\chi = 2.75$

The paraboloid $\mathbb{P}^2$

- Paraboloid $\mathbb{P}^2 = \{x \in \mathbb{R}^3 : x_0 = x_1^2 + x_2^2\}$
  - $\mathbb{P}^2$ is a singular limit case ($\alpha = \pi/4$) between
    - the sphere $\mathbb{S}^2$ ($\alpha = 0$) and ellipsoids ($0 < \alpha < \pi/4$)
    - the two-sheeted hyperboloids ($\alpha > \pi/4$)
  - Missing ingredient : $\mathbb{P}^2$ has no large isometry group
  - $\mathbb{P}^2$ does not have a constant curvature

$\Longrightarrow$ general method does not work, designing a CWT on $\mathbb{P}^2$ is hard!

CWT on the paraboloid $\mathbb{P}^2$: Suggestions

Suggestions

(1) Consider the related manifold : $\mathfrak{P} = \mathbb{P}^2 \setminus \{0,0,0\}$, paraboloid with apex removed

- The set P of 3×3 matrices of the form $g = \mathrm{diag}(a^2, ar_\theta)$, whith $a > 0$, $r_\theta \in$SO(2), leaves both $\mathbb{P}^2$ and $\mathfrak{P}$ invariant !
- Embed P into the group

$$\mathrm{G} = \left\{ g(\mathbf{b}, a, \theta) \equiv \begin{pmatrix} a^2 & \mathbf{0}^T \\ \mathbf{b} & ar_\theta \end{pmatrix} : a > 0, \mathbf{b} \in \mathbb{R}^2, 0 \leqslant \theta < 2\pi \right\}$$

G = nonunimodular Lie group, similar to, but different from SIM(2)

- Then P $\simeq$ G/H $\simeq \mathfrak{P}$, where H $= \{g(\mathbf{b}, a, \theta) : a = 1, \theta = 0\}$
  - P has a natural action on $\mathfrak{P}$
  - There is a P-invariant measure on $\mathfrak{P}$
- G has a unique UIR U in $L^2(\mathfrak{P}, d\mu_{\mathfrak{P}})$ and it is square integrable
Corresponding "coherent states" :

$$\psi_{\mathbf{b},a,\theta} = (c_\psi)^{-1/2}\, U(\mathbf{b}, a, \theta)\psi, \quad (\mathbf{b}, a, \theta) \in \mathrm{G}$$

- The corresponding time-frequency transform looks more like a Gabor transform than a wavelet transform !

CWT on the paraboloid $\mathbb{P}^2$: Suggestions

(2) Transport a CWT from cylinder to $\mathfrak{P}$

- Set-up a CWT on cylinder

$$\mathbb{Z} = \left\{ X(x_0, \theta) = (x_0, \cos\theta, \sin\theta)^T : x_0 \in \mathbb{R}, 0 \leqslant \theta < 2\pi \right\}$$

w.r. to group $\mathrm{G}_3 = \mathrm{G}_{\mathrm{aff}} \times \mathrm{SO}(2)$ with action

$$X(x_0, \theta) \mapsto X(g(x_0, \theta)) = X(ax_0 + b, \theta + \phi \bmod 2\pi), \; g = (a, b, \phi) \in \mathrm{G}_3$$

- define CWT as usual
- transport that CWT from $\mathbb{Z}$ to $\mathfrak{P}$ by homeomorphism
- get CWT on $\mathfrak{P}$

- Problems :
  - Group G_3 too small, no irreducible representation in $L^2(\mathbb{Z}, dx_0 d\theta)$
  - $\mathrm{G}_3 \ni g(a, 0, 0) \neq$ genuine 2-D dilation : it dilates only in the x_0 direction

    $\Rightarrow$ not a genuine CWT !
  - the same is true for CWT on $\mathfrak{P}$
- Conclusion : this approach does not respect the geometry of the problem (the cylinder is flat !), not sufficient !

CWT on the paraboloid $\mathbb{P}^2$: Suggestions

(1-2) [S.T.Ali & G.Honnouvo, Concordia U., Montréal]

(3) Same method as for $\mathbb{S}^2$ [D.Roşca & JPA]

- Start from orthogonal wavelet basis in the plane $x_0 = 0$
- Lift it to $\mathbb{P}^2$ with inverse vertical projection
- Get orthogonal wavelet basis in $L^2(\mathbb{P}^2, ds)$ (work in progress)

The CWT on the conic sections: A unified approach

[I. Bogdanova and P. Vandergheynst (EPFL), JPA]

- All conic sections are obtained as sections of a double null-cone

$$\mathcal{C}_0^3 = \{(x_0, x_1, x_2, x_3) \in \mathbb{R}^4 : \; x_0^2 - x_1^2 - x_2^2 - x_3^2 = 0\}$$

by a hyperplane $x_0 = 1 + \tan\alpha(x_3 - 2)$, $0 \leqslant \alpha \leqslant \pi/2$.

- Analogy : intersection of 3-dimensional cone $\mathcal{C}_0^2$ with plane

$$x_0 = 1 + \tan\alpha(x_3 - 1), \; 0 \leqslant \alpha \leqslant \pi/2$$

For $\alpha = \pi/4$: degenerate paraboloid (half-line)

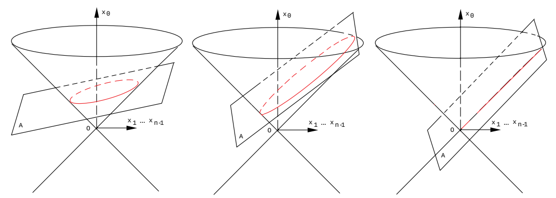

Construction of dilations

- On any section, define generalized projective coordinates

$$u_i = \frac{1 - 2\tan\alpha}{x_0 - x_3 \tan\alpha}\, x_i, \;\; i = 1, 2, 3$$

For the sphere $(\alpha = 0)$: $u_i = x_i / x_0$

- Dilation = Lorentz boost of parameter $t \in \mathbb{R}$ along axes x_0, x_3
- Result :

$$u_i' = u_i, \;\; i = 1, 2$$

$$u_3' = \frac{(1 - 2\tan\alpha)(u_0 \sinh t + u_3 \cosh t)}{u_0 \cosh t + u_3 \sinh t + \tan\alpha (u_0 \sinh t + u_3 \cosh t)},$$

where $u_0 = 1 + \tan\alpha (u_3 - 2)$

For the sphere $(\alpha = 0)$:
recover stereographic dilation $\tan\frac{\theta_a}{2} = a \tan\frac{\theta}{2}$, with $a = e^t$

Construction of dilations

Dilation on the sphere or an ellipsoid via Lorentz boost

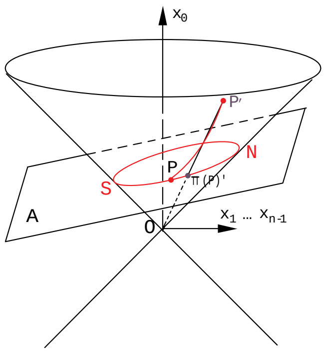

Graphically :

- S,N = South, resp. North, pole of sphere or ellipsoid
- boost $P \mapsto P'$
- back to sphere by homogeneous coordinates $P' \mapsto \pi(P')$

Construction of conic sections

- Group-theoretical generation of conic sections :
  - Start from spherical section $x_0 = 1$
  - Apply boost along $x_0, x_2 \;\Rightarrow\;$ get ellipsoid of revolution around x_0 axis
  - Start from hyperbolic section $x_3 = 1 \;\Rightarrow\;$ get 2-sheeted hyperboloid
  - As limit from both sides, paraboloid becomes degenerate half-line (see previous figure)
- Differential-geometric generation of conic sections :
  - upper sheet of null-cone $\mathcal{C}_0^3$ without tip = trivial principal fiber bundle with base $\mathbb{S}^2$ (spherical section) and fiber $\mathbb{R}$
  - sections of $\mathcal{C}_0^3$ by various planes = global C^∞ sections in that fiber bundle (in differential geometry sense)

The CWT on conic sections

- Strategy for building CWT :
  - Start with spherical section that gives $\mathbb{S}^2$ and consider the usual representation U of the Lorentz group $\mathrm{SO}_o(1,3)$ in $L^2(\mathbb{S}^2)$
  - Any other smooth section $\sigma : \mathbb{S}^2 \to \mathcal{C}_0^3$ of the same type
    - allows to bring the action of $\mathrm{SO}_o(1,3)$ to $\sigma(\mathbb{S}^2)$
    - induces an isometry $V_\sigma : L^2(\mathbb{S}^2) \to L^2(\sigma(\mathbb{S}^2))$
  - Get a new UIR of $\mathrm{SO}_o(1,3)$ in $L^2(\sigma(\mathbb{S}^2))$ by $V \circ U \circ V^{-1}$
  - Then the construction of wavelets on the new section is immediate
  - Same technique starting from hyperbolic section giving $\mathbb{H}^2$
- Conclusion :
  - Promising approach
  - Much work remains to be done !
    (in progress : S.T.Ali, P.Vandergheynst, D. Roşca, JPA)

REFERENCES

References

General references

- I. Daubechies *Ten Lectures on Wavelets*, SIAM, Philadelpia, 1992
- B. Torrésani, *Analyse continue par ondelettes*, InterÉditions/CNRS Éditions, Paris, 1995
- S.G. Mallat, *A Wavelet Tour of Signal Processing*, 2nd ed., Academic Press, San Diego, 1999
- J-P. Antoine, R. Murenzi, P. Vandergheynst and S.T. Ali, *Two-dimensional Wavelets and Their Relatives*, Cambridge Univ. Press, Cambridge (UK), 2004
- Wavelet Toolbox YAWTb: `http://rhea.tele.ucl.ac.be/yawtb/`

References on wavelet analysis on the sphere and other conic sections

- J-P. Antoine and P. Vandergheynst, Wavelets on the 2-sphere: A group-theoretical approach, *Applied Comput. Harm. Anal.* **7** (1999) 262–291
- J-P. Antoine and P. Vandergheynst, Wavelets on the *n*-sphere and other manifolds, *J. Math. Phys.* **39** (1998) 3987–4008

- J-P. Antoine, L. Demanet, L. Jacques, and P. Vandergheynst, Wavelets on the sphere: Implementation and approximations, *Applied Comput. Harmon. Anal.* **13** (2002) 177–200
- I. Bogdanova, P. Vandergheynst, J-P. Antoine, L. Jacques, and M. Morvidone, Stereographic wavelet frames on the sphere, *Applied Comput. Harmon. Anal.* **26** (2005) 223–252
- Y. Wiaux, L. Jacques, and P. Vandergheynst, Correspondence principle between spherical and Euclidean wavelets, *Astrophys. J.* **632** (2005) 15–28
- I. Bogdanova, P. Vandergheynst, and J-P. Gazeau, Continuous wavelet transform on the hyperboloid, *Applied Comput. Harmon. Anal.* (2007), **23** (2007) 285–306
- J-P. Antoine and P. Vandergheynst, Wavelets on the two-sphere and other conic sections, *J. Fourier Anal. Appl.* **13** (2007) 369–386
- J-P. Antoine, I. Bogdanova, and P. Vandergheynst, The continuous wavelet transform on conic sections, *Int. J. Wavelets, Multires. and Inform. Proc.* **6** (2007) 137–156
- J-P. Antoine and D. Roşca, The wavelet transform on the two-sphere and related manifolds — A review, *Optical and Digital Image Processing*, Proc. SPIE, vol. 7000 (2008) (to appear)